Published May 11, 2009

mice for tumor destruction with the combination therapy, although the antitumor effects became significant compared with gemcitabine alone 40 d after combined therapy even with $CD8^+$ T cell depletion (Fig. 3 B). These findings suggest that the cell autonomous modes of tumor cell killing with MFG-E8 blockade are not sufficient to maintain durable control of the established cancers. Consistent with a key role for T cells in the generation of long-lived and specific protective immunity, treated mice rejected a subsequent lethal challenge with MC38 tumor cells but not B16 melanoma or MCA-205 fibrosarcoma cells (Fig. 3 C).

To characterize the T cell responses stimulated with treatment, we isolated tumor-infiltrating lymphocytes from regressing MC38 lesions. Although the proportions of total $CD4^+$ and $CD8^+$ T cells did not vary as a function of therapy, anti–MFG-E8 antibodies alone or in combination with CPT-11 significantly reduced the numbers of intratumoral $Foxp3^+$ T reg cells (Fig. 4 A). Although chemotherapy alone had no impact on T reg cell numbers, combined treatment with anti–MFG-E8 antibodies decreased T reg cell numbers in the spleen as well (Fig. 4 A). The T reg cells that were recovered after MFG-E8 blockade, however, did not manifest impaired function on a per cell basis, as assessed in standard in vitro suppression assays (unpublished data). These findings extend our earlier demonstration that MFG-E8 is an important determinant of antitumor T reg cell numbers (10, 12).

The combination treatment, but not anti–MFG-E8 antibodies alone, markedly increased $CD4^+$ and $CD8^+$ effector T cell activation and function. This stimulation resulted in high levels of surface CD44, IFN-γ production, and tumor-specific cytotoxicity (Fig. 4, B–D). The combination therapy also augmented the total levels of circulating IgG2a and IgG2b antibodies, which might contribute to tumor destruction through Fc-dependent cytotoxicity (Fig. S3). These results highlight the synergy between systemic MFG-E8 blockade and chemotherapy for boosting multiple antitumor effector mechanisms.

Anti–MFG-E8 antibodies enhance dendritic cell cross-presentation of tumor antigens

Because MFG-E8 promotes the uptake of apoptotic cells by mononuclear phagocytes (10, 19–21), we next characterized the impact of chemotherapy and MFG-E8 blockade on

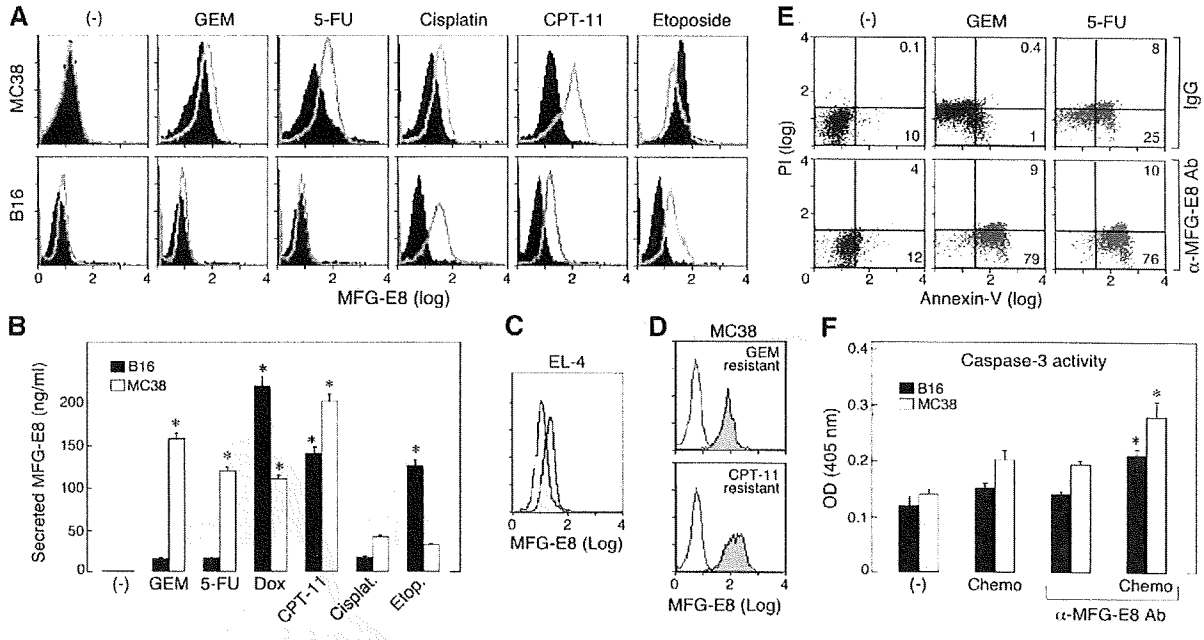

Figure 2. Drug-resistant tumor cells express MFG-E8. (A) MC38 carcinoma and B16 melanoma cells were treated with various cytotoxic agents under serum-free condition for 24 h, and intracellular MFG-E8 expression in viable cells (annexin V^-/propidium $iodide^-$) was determined with flow cytometry. The shaded and open histograms represent the levels of expression on untreated and treated cells, respectively. Gemcitabine (GEM) and 5-FU accomplished minimal killing of B16 cells (not depicted). (B) MFG-E8 levels in culture supernatants from A were measured with ELISA. (C) EL-4 thymoma cells were treated with γ irradiation (100 Gy), and MFG-E8 expression in viable cells (annexin V^-/propidium $iodide^-$) was determined with flow cytometry. (D) Stable drug-resistant variants of MC38 were generated and tested for MFG-E8 expression with flow cytometry (shaded histogram). The staining with isotype control antibodies is also shown. (E) MC38 carcinoma cells were exposed to GEM or 5-FU in the presence of anti–MFG-E8 mAb or isotype control as in A, and cell viability was determined with flow cytometry (percentages are shown). (F) Established MC38 and B16 tumors (25 mm^2) were treated with GEM or dacarbazine, respectively, with or with systemic anti–MFG-E8 mAb as in Fig. 1. 4 d after completion of therapy, tumor homogenates were prepared and assayed for caspase 3 activation with ELISA. Presented data are representative of three independent experiments with similar results. Means ± SEM are shown in B and F. *, $P < 0.05$ between the treatment and control.

Published May 11, 2009

antigen-presenting cells. Although the combination treatment did not influence the proportions of macrophages ($CD11b^+$ $Gr\text{-}1^-$) or myeloid-derived suppressor cells ($CD11b^+$ $Gr\text{-}1^+$) that were isolated from regressing MC38 colon tumors (Fig. S4), the numbers of $CD11b^+$, $CD11c^+$ dendritic cells were significantly increased, and these cells expressed high levels of the co-stimulatory molecule CD86 (Fig. 5 A). As bone marrow–derived dendritic cells (BMDCs) efficiently phagocytosed chemotherapy-exposed MC38 and B16 cells in vitro (Fig. S5),

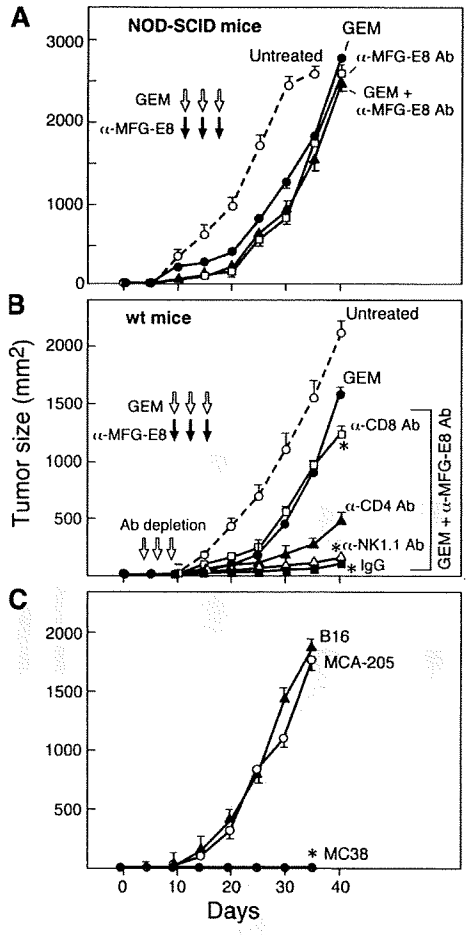

Figure 3. The therapeutic activity of MFG-E8 antibody blockade and chemotherapy involves host immunity. (A) NOD-SCID mice harboring established MC38 carcinomas (25 mm^2) were treated with systemic gemcitabine (GEM) and anti-MFG-E8 mAb. (B) Established MC38 carcinomas bearing wild-type C57BL/6 mice that were depleted of $CD4^+$, $CD8^+$, or $NK1.1^+$ cells with antibodies were treated with systemic GEM and anti-MFG-E8 mAb. (C) Wild-type C57BL/6 mice that had rejected established MC38 carcinomas with systemic GEM and anti-MFG-E8 mAb showed specific long-term protective immunity against subsequent challenge with MC38 cells during the follow-up period (>200 d). Each experiment was performed with five mice per group, and similar results were observed for each panel in three independent experiments. Shown are the means ± SEM for each cohort in a representative experiment. *, $P < 0.05$ between the treatment and control.

our analysis of the tumor infiltrates raised the possibility that dendritic cell capture of tumor cells in situ might be important for T cell priming.

To study the impact of anti–MFG-E8 antibodies on dendritic cell cross-presentation in more detail, we used EL-4 thymoma cells engineered to express OVA (EG.7-OVA) (22) and the syngeneic C57BL/6 mice harboring a transgenic TCR specific for an MHC class II–presented OVA peptide (OT-II) (23). BMDCs efficiently ingested irradiated EG.7-OVA cells, and this was only minimally blocked by an antibody to α_v integrins or MFG-E8, indicating that this pathway was not required for tumor cell uptake in this system (Fig. 5 B and not depicted). Although anti–MFG-E8 antibodies did not affect the overall phagocytosis of irradiated EG.7-OVA cells, a blocking antibody to Fc receptors but not to α_v integrins partially attenuated uptake. These results reveal that anti–MFG-E8 antibodies switch the receptor for MFG-E8–mediated tumor cell ingestion from $\alpha_v\beta_3/\alpha_v\beta_5$ integrins to Fc receptors.

Consistent with the ability of activating Fc receptors to trigger immune stimulation (24), the opsonization of EG.7-OVA cells with anti–MFG-E8 antibodies enhanced dendritic cell stimulation of OT-II TCR transgenic $CD4^+$ T cells. This activation resulted in increased production of IFN-γ (Fig. 5 C) but not IL-4 or IL-17 (not depicted). In contrast, anti-Fc receptor antibodies inhibited cross-priming, whereas anti-α_v integrin antibodies augmented T cell responses when either irradiated EG.7-OVA cells alone or anti–MFG-E8 antibody opsonized, irradiated EG.7-OVA cells were fed to dendritic cells (Fig. 5 C). The anti–MFG-E8 antibodies also increased cross-presentation to MHC class I–restricted OT-I $CD8^+$ T cells, resulting in increased IFN-γ production (Fig. S6). Collectively, these findings suggest that MFG-E8 blockade enhances Th1 antitumor responses.

To further examine the importance of MFG-E8 antibody–mediated cross-priming in vivo, we injected irradiated EG.7-OVA cells together with anti–MFG-E8 antibodies into the footpads of OT-I mice and measured OVA-specific T cell responses in the draining lymph nodes 5 d later. In some experiments, blocking anti-FcγR antibodies were coadministered to evaluate the role of FcR-mediated uptake for antigen presentation. Although the injection of anti–MFG-E8 antibodies enhanced specific $CD8^+$ T cell IFN-γ production, the concurrent administration of anti-FcγR antibodies substantially inhibited this response (Fig. 5 D). These results indicate that MFG-E8 blockade promotes cross-priming of antigen-specific $CD8^+$ T cells primarily through FcR-mediated antigen uptake.

MFG-E8 modulates dendritic cell cytokine production

To further clarify the mechanisms underlying T cell stimulation, we examined the impact of MFG-E8 on dendritic cell cytokine production after the uptake of dying tumor cells. The addition of rMFG-E8 protein increased dendritic cell IL-10 secretion, whereas anti–MFG-E8 antibodies reduced IL-10 but enhanced IL-12, IL-23, and TNF-α production (Fig. 6 A). The effects of MFG-E8 on cytokine profiles were blocked with the RMV-7 anti-α_v integrin antibody (unpublished data), confirming the importance of $\alpha_v\beta_3$ and $\alpha_v\beta_5$ integrins in this response.

Published May 11, 2009

To address the role of IL-12 in the immune stimulation with anti–MFG-E8 antibodies, we used IL-12p35–deficient mice in a series of in vivo and in vitro studies. The efficacy of anti–MFG-E8 antibodies and CPT-11 treatment against MC38 colon tumors was partially reduced in IL-12–deficient mice compared with wild-type controls (Fig. 6 B). Moreover, the anti–MFG-E8 antibody–mediated cross-presentation of EG.7-OVA cells to OT-II $CD4^+$ T cells was slightly decreased with IL-12–deficient dendritic cells compared with wild-type controls (Fig. 6 C). These results suggest that IL-12 contributes to the anti–MFG-E8 antibody–triggered immunostimulation, but other cytokines and/or cell-surface molecules also play important roles.

DISCUSSION

Although substantial evidence demonstrates that cross talk between tumor cells and normal host elements is critical to carcinogenesis (25), most cancer therapies primarily target individual compartments. Small molecule inhibitors of oncogenic tyrosine kinases and antibody blockade of VEGF serve as prototypes of rationally designed agents that antagonize major pathogenic mechanisms in cancer cells and the host, respectively (26, 27). Although these treatments afford important clinical benefits, most patients achieve only partial responses and eventually succumb to progressive disease caused by the emergence of drug-resistant variants. However, analogous to the ways in which antimicrobial agents cooperate with host reactions to effectuate sterilizing immunity for some serious infections (28), cancer treatments might be significantly improved through concurrently targeting the tumor and host. The results presented in this paper illustrate the potential for systemic MFG-E8 antibody blockade in combination with conventional oncologic therapies to accomplish this dual targeting.

MFG-E8 promotes cancer progression through coordinated $\alpha_v\beta_3$ integrin signaling in tumor cells, vascular elements, and infiltrating myeloid cells (12). Although the administration of anti–MFG-E8 antibodies alone resulted in only modest tumor destruction and immune stimulation, the coupling

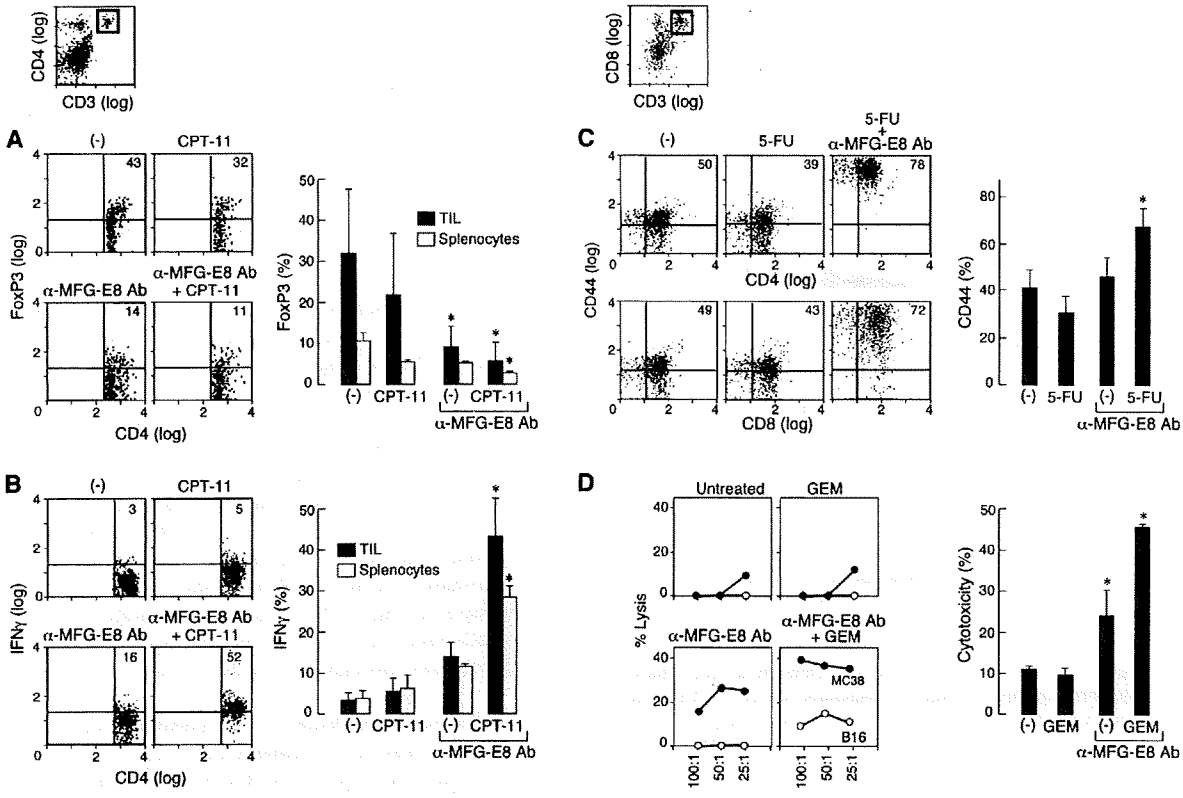

Figure 4. Combination MFG-E8 antibody blockade and chemotherapy enhances antitumor effector T cells and inhibits FoxP3⁺ T reg cells. Tumor-infiltrating lymphocytes (TILs) were harvested from mice bearing MC38 tumors 5 d after the indicated treatment. The TILs were gated as $CD3^+CD4^+$ or $CD3^+CD8^+$ T cells, and assayed for (A) FoxP3, (B) IFN-γ, and (C) CD44 expression with flow cytometry (percentages are shown). Representative stainings are presented. The means ± SEM for six mice per group are shown in the adjacent panels. (D) Draining lymph nodes were harvested from MC38-bearing mice after the indicated treatments and evaluated for cytotoxic activity against ^{51}Cr-labeled MC38 and B16 targets in vitro. The percent specific lysis is presented. Each experiment was independently performed four times. The means ± SEM at an effector/target ratio of 100:1 for six mice per group are shown in the adjacent panels. *, $P < 0.05$ between the treatment and control.

Published May 11, 2009

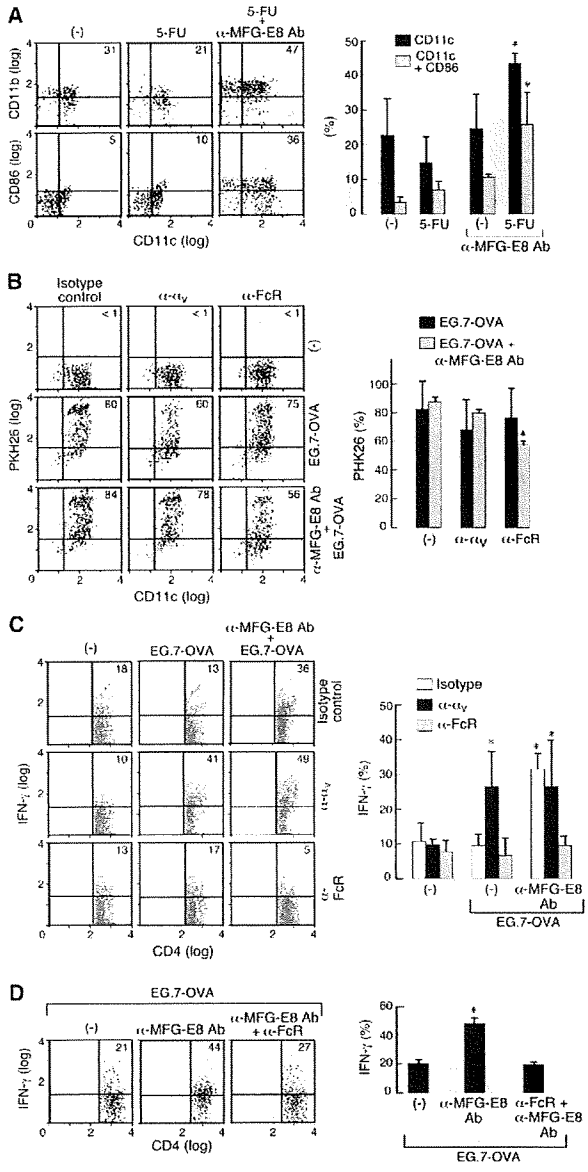

Figure 5. Anti–MFG-E8 antibodies enhance dendritic cell cross-presentation of dying tumor cells. (A) Tumor-infiltrating cells were harvested from mice harboring MC38 carcinomas 4 d after the indicated treatment. The $CD3^+$ and $B220^+$ lymphocytes were excluded by gating, and the remaining forward/side scatter high cells were analyzed for CD11c, CD11b, and CD86 with flow cytometry (percentages are shown). Similar results were observed in three experiments. Shown to the right are the means ± SEM for five mice per group. *, $P < 0.05$. (B) BMDCs were co-cultured with PKH26-labeled EG.7-OVA cells (with or without opsonization with anti–MFG-E8 mAbs) and evaluated for phagocytosis. The impact of blocking antibodies to α_v integrins and Fc receptors was determined (percentages are shown). Similar results were observed in three experiments, and the means ± SEM are shown. *, $P < 0.05$. (C) BMDCs that were loaded with EG.7-OVA cells as in B were co-cultured with OVA-specific TCR transgenic $CD4^+$ T cells, and IFN-γ production was evaluated with flow cytometry (percentages are shown). The effects of anti-α_v integrin and Fc receptor antibodies are shown. Similar results were observed in three experiments, and the means ± SEM are shown to the right. *, $P < 0.05$. (D) 10^5 irradiated EG.7-OVA cells per mouse were injected into the footpads of OT-I mice with anti–MFG-E8, anti-FcγR, and isotype control antibodies as indicated. The draining lymph nodes were harvested after 5 d, and $CD8^+$ T cell IFN-γ production was determined with flow cytometry (percentages are shown). Similar results were observed in three experiments. Shown are the means ± SEM. *, $P < 0.05$.

of drug-induced tumor cell death to MFG-E8 blockade effectuated the sustained regressions of established colon carcinomas, melanomas, and lymphomas. A key component of this therapeutic synergy is the ability of anti–MFG-E8 antibodies to attenuate tumor cell resistance to cytotoxic treatments, likely because of the inhibition of Akt activation. Some degree of intrinsic tumor cell sensitivity to the cytotoxic agent appears necessary for this enhancement, though, because gemcitabine, which failed to provoke B16 cell death in vitro (unpublished data), proved inactive in vivo in combination with MFG-E8 blockade. An additional mechanism by which anti–MFG-E8 antibodies might increase tumor cell killing, particularly in conjunction with anti–VEGFR-2 antibodies, may involve a more robust inhibition of the tumor blood supply, as MFG-E8 is required for VEGF-induced angiogenesis (14, 18). Moreover, knockdown of MFG-E8 in MC38 carcinoma cells exposed to chemotherapy also reduced VEGF production (unpublished data).

Upon the induction of tumor cell death in vivo with cytotoxic treatments, MFG-E8 blockade favored the establishment of an immunogenic tumor microenvironment. This conversion reflected the dual capacity of anti–MFG-E8 antibodies to antagonize $\alpha_v\beta_3$ integrin–driven immune suppression and to promote efficient Fc receptor–mediated dendritic cell cross-presentation. In this context, recent analysis of mice harboring a myeloid cell–specific KO of α_v integrins has underscored the importance of this receptor in attenuating inflammation (29), perhaps through the induction of Twist (12), an antagonist of the NF-κB pathway (30). Consistent with these results, we found that MFG-E8 blockade resulted in increased IL-12 production. This proinflammatory cytokine contributed to tumor protection, as revealed through studies of p35-deficient mice, although other factors such as IL-23, TNF-α, and type I IFNs may play important roles as well. Accumulating evidence has also highlighted the ability of mAbs to opsonize tumor cells for efficient cross-presentation by dendritic cells, thereby engendering potent antitumor immunity (31). Collectively, these factors may promote the development of dense intratumoral infiltrates composed of abundant $CD4^+$ and $CD8^+$ effector T cells but only limited $FoxP3^+$ T reg cells. It is tempting to speculate that this broad T cell response may suppress the emergence of drug-resistant tumor cells and mediate long-term protection against tumor recurrence. In accordance with this idea, previous experimental and clinical studies have shown that a high ratio of effector T cells to T reg cells is tightly linked with sustained tumor destruction (32, 33).

Published May 11, 2009

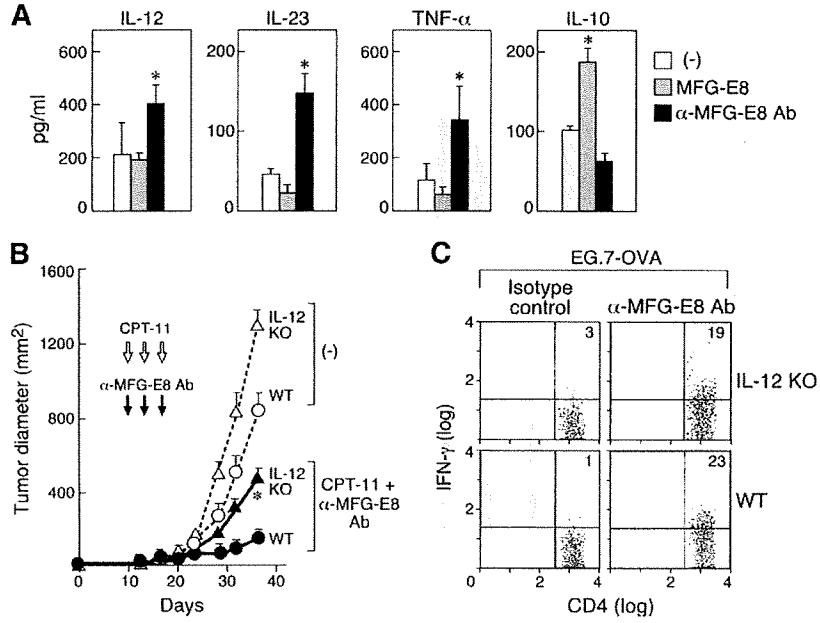

Figure 6. Anti–MFG-E8 antibodies modulate antigen-presenting cell cytokine profiles. (A) BMDCs were treated with recombinant MFG-E8 or anti–MFG-E8 mAbs, and cytokine production was determined with ELISA. Shown are the means ± SEM for three experiments. *, $P < 0.05$. (B) C57BL/6 wild-type or IL-12p35-deficient mice harboring established MC38 colon carcinomas (25 mm^2) were treated with systemic gemcitabine with or without anti–MFG-E8 mAb, as shown in Fig. 1 A. Shown are the means ± SEM for five mice per group. Similar results were observed in a second experiment. *, $P < 0.05$ between treated wild-type and IL-12 KO mice. (C) BMDCs from wild-type or IL-12–deficient mice were loaded with EG.7-OVA cells and co-cultured with $CD4^+$ T cells obtained from wild-type mice that were immunized with EG.7-OVA cells (five times). IFN-γ production was evaluated by flow cytometry (percentages are shown). Similar results were observed in a second experiment.

Recent work has illustrated that some cytotoxic therapies, including anthracyclines and taxanes, may induce a form of immunogenic cell death in which the release of calreticulin and high mobility group box 1 from dying tumor cells serves as an innate activating signal (34–36). Cytotoxic therapies may additionally trigger the DNA damage response to up-regulate tumor cell expression of NKG2D ligands, thereby eliciting NK and $CD8^+$ T cell responses (37). Moreover, agonistic antibodies to TNF-related apoptosis-inducing ligand receptors, which are frequently expressed on cancer cells, mediate potent antitumor effects in association with other immunotherapies (38, 39). Our results elucidate several novel antitumor mechanisms through which systemic MFG-E8 blockade may potentiate the efficacy of conventional oncologic therapies by coordinately targeting tumor cells and components of the tumor microenvironment. Perhaps the coupling of anti–MFG-E8 antibodies to tumor cell death might be considered a new strategy for in vivo cancer vaccination.

MATERIALS AND METHODS

Mice. C57BL/6, NOD-SCID, and OVA transgenic OT-II mice were obtained from SRL or the Jackson Laboratory and housed under specific pathogen-free conditions. OT-I and IL-12p35 gene KO mice were used as previously described (40, 41). All experiments were conducted according to a protocol approved by the review committee of animal research at the Institute of Medical Sciences of the University of Tokyo or Keio University School of Medicine.

In vivo tumor challenges. 6-wk-old C57BL/6, NOD-SCID, or IL-12 KO female mice were injected intradermally with 10^5 MC38 colon carcinoma, B16 melanoma, EL-4 thymoma, or MCA205 fibrosarcoma cells. After the tumors grew to an approximate size of 25 mm^2, the mice were treated with various therapeutic regimens. For the MC38 tumors, mice received on days 10, 12, and 14 1 or 4 mg/ml gemcitabine, 5 mg/ml 5-FU, 1 mg/ml CPT-11, 40 mg/ml of the VEGFR-2 mAb DC101 (ImClone Systems), or the 40 mg/ml of the EGFR tyrosine kinase inhibitor AG490 (MERCK). In some experiments, tumors were treated with five daily doses of irradiation (3 Gy at a rate of 4 Gy/min) using an isolator system. For the B16 tumors, mice were treated with 5 mg/ml doxorubicin, 2 mg/ml etoposide, or gemcitabine as described. For EL-4 thymoma cells, mice were treated with 5 mg/ml doxorubicin, as described. A hamster mAb against MFG-E8[1] (at 2 mg/ml; MBL International), an isotype control immunoglobulin IgG2a, or 1 mg/ml of rabbit polyclonal anti–MFG-E8 sera (provided by C. Thèry, Institut National de la Santé et de la Recherche Médicale, Paris, France) (17, 18) were administered concurrently with the cytotoxic therapies. In some studies, mice were also treated with depleting antibodies against CD4 (clone GK1.5), CD8 (clone 53-6.72), and NK1.1 (PK-136; American Type Culture Collection) at days −5, −3, and 0 relative to the cytotoxic therapy (40, 42). Tumor growth was monitored regularly and the products of the perpendicular diameters were recorded.

Apoptosis assays. Tumor cells were cultured in serum-free media and treated with various cytotoxic agents overnight with or without anti–MFG-E8 antibodies. To generate stable drug-resistant variants, MC38 cells were cultured in gradually increasing concentrations of gemcitabine (from 1 to 20 μg/ml) or CPT-11 (from 0.5 to 10 μg/ml) over ~8 wk. MFG-E8 expression was measured by flow cytometry using the hamster anti–MFG-E8 mAb followed by an anti-mouse IgG, as previously described (10). Secreted MFG-E8 levels

Published May 11, 2009

were measured with an ELISA according to the manufacture's instruction (R&D Systems). Cell death was determined with annexin V and propidium iodide staining, or DiOC6 labeling to quantify the mitochondrial membrane potential, according to the manufacturer's instructions (BD). To measure tumor apoptosis in vivo, we treated established MC38 or B16 tumors (25 mm^2) with 10 mg/ml gemcitabine or dacarbazine with or without anti–MFG-E8 antibodies, harvested the tumors 4 d after therapy, and measured caspase 3 activation in tumor homogenates with a colorimetric assay kit (Invitrogen).

Immune assays. Tumor-infiltrating lymphocytes were harvested with a cell gradient separation (Nocoprep; Axis-Shield), as previously described (10). Cell populations were characterized using mAbs against CD3, CD4, CD8, CD11b, CD11c, CD44, CD86, Gr-1, and Foxp3 (clone MF23). IFN-γ production was measured by intracellular flow cytometry, as previously described (10). Cytotoxicity was measured by incubating lymphoid cells isolated from draining lymph nodes with irradiated MC38 cells for 96 h and then testing lytic activity against ^{51}Cr-labeled MC38 and B16 targets. The percent lysis was calculated as (experimental − spontaneous)/(maximum − spontaneous) × 100, using 5% Triton X and medium alone for determination of the maximum and spontaneous counts.

BMDCs were cultured from bone marrow precursors using GM-CSF–conditioned media for 7 d and were then treated with 100 ng/ml of recombinant MFG-E8 (R&D Systems), 20 μg/ml anti–MFG-E8 mAb (MBL International), or 20 μg/ml of polyclonal MFG-E8 antiserum overnight. Culture supernatants were evaluated for IL-12, IL-23, TNF-α, and IL-10 levels with ELISAs.

Cross-priming assays. Day 7 BMDCs were also co-cultured with irradiated EG.7-OVA cells (1:10 ratio) that were labeled with PKH26 (Sigma-Aldrich) in 12-well round-bottom plates, and phagocytosis was determined with flow cytometry. In some experiments, the tumor cells were pretreated with 30 mg/ml anti–MFG-E8 mAb for 30 min before the co-culture. The impact of blocking antibodies to α_v integrins (clone RMV-7; Millipore) or Fc receptors (clone 2.4G2; BD) on tumor cell uptake was similarly evaluated. To antigen presentation by DCs, naive $CD4^+$ T cells were isolated from the spleens of OT-I or OT-II mice by magnetic cell sorting (Miltenyi Biotec) and added to the tumor cell–loaded dendritic cells for 24 h. Intracellular IFN-γ expression in T cells was then determined by flow cytometry.

For in vivo cross-priming assays, 10^6 irradiated EG.7-OVA cells per mouse were injected into the footpads of OT-I mice with 1 mg/ml anti–MFG-E8 mAb, 1 mg/ml anti-FcR blocking antibody (clone 2.4G2), or isotype control. 5 d after the challenge, mice were sacrificed, and the draining lymph node cells were isolated and cultured with 10 mg/ml MHC class I–restricted OVA peptides overnight. IFN-γ production by $CD8^+$ T cells was then determined by flow cytometry or ELISA using the culture supernatants.

Statistical analysis. Statistical analysis was performed using the unpaired Student's *t* test or one-way analysis of variance through all of the experimental procedures. Differences were considered significant when the p-value was <0.05.

Online supplemental material. Fig. S1 associates temporal relationships of anti–MFG-E8 antibody and chemotherapy administration in antitumor responses. Fig. S2 presents in vivo antitumor activities of anti–MFG-E8 antibody and doxorubicin against established EL-4 thymomas. Fig. S3 shows the humeral responses induced by in vivo treatment of anti–MFG-E8 antibody and chemotherapy. Fig. S4 shows the frequency of $CD11b^+$ and $CD11b^+$ $Gr\text{-}1^+$myelid cells at tumors with the treatments. Fig. S5 suggests the in vitro phagocytosis of apoptotic tumor cells by BMDCs. In Fig. S6, the effect of anti–MFG-E8 antibody was examined in mediating in vitro cross-presentation of OVA antigen to OT-I T cells by BMDCs. Online supplemental material is available at http://www.jem.org/cgi/content/full/jem.20082614/DC1.

We wish to thank Dr. Clotilde Thery for valuable advice in the making of rabbit polyclonal antibody against mouse MFG-E8; A. Tuross for her secretarial assistance; and S. Hatayama, A. Asami and R. Mivake for assistance with the in vivo tumor study, ELISA assay, and animal care. M. Jinushi, G. Dranoff, and H. Tahara were responsible for experimental design; M. Jinushi, M. Sato, and S. Nagai were responsible for the preparation and performance of experiments; data analysis and interpretation were performed by M. Jinushi, M. Sato, A. Kanamoto, A. Itoh, S. Nagai, S. Koyasu, G. Dranoff, and H. Tahara; and M. Jinushi, G. Dranoff, and H. Tahara prepared the manuscript.

This study was supported in part by the Grants-in-Aid for Scientific Research on Priority Areas (20015016 to H. Tahara) and for Young Scientists (Start-Up; 20890050 to M. Jinushi) from the Ministry of Education, Culture, Sports, Science and Technology of Japan, as well as by the Melanoma Research Alliance and the Research Foundation for the Treatment of Ovarian Cancer (G. Dranoff).

The authors have no conflicting financial interests.

Submitted: 19 November 2008
Accepted: 17 April 2009

REFERENCES

1. Dranoff, G. 2004. Cytokines in cancer pathogenesis and cancer therapy. *Nat. Rev. Cancer.* 4:11–22.
2. de Visser, K.E., A. Eichten, and L.M. Coussens. 2006. Paradoxical roles of the immune system during cancer development. *Nat. Rev. Cancer.* 6:24–37.
3. Balkwill, F., K.A. Charles, and A. Mantovani. 2005. Smoldering and polarized inflammation in the initiation and promotion of malignant disease. *Cancer Cell.* 7:211–217.
4. Smyth, M.J., G.P. Dunn, and R.D. Schreiber. 2006. Cancer immunosurveillance and immunoediting: the roles of immunity in suppressing tumor development and shaping tumor immunogenicity. *Adv. Immunol.* 90:1–50.
5. Karin, M., and F.R. Greten. 2005. NF-kappaB: linking inflammation and immunity to cancer development and progression. *Nat. Rev. Immunol.* 5:749–759.
6. Yu, H., M. Kortylewski, and D. Pardoll. 2007. Crosstalk between cancer and immune cells: role of STAT3 in the tumour microenvironment. *Nat. Rev. Immunol.* 7:41–51.
7. Rakoff-Nahoum, S., and R. Medzhitov. 2007. Regulation of spontaneous intestinal tumorigenesis through the adaptor protein MyD88. *Science.* 317:124–127.
8. Naugler, W.E., T. Sakurai, S. Kim, S. Maeda, K. Kim, A.M. Elsharkawy, and M. Karin. 2007. Gender disparity in liver cancer due to sex differences in MyD88-dependent IL-6 production. *Science.* 317:121–124.
9. Jinushi, M., F.S. Hodi, and G. Dranoff. 2008. Enhancing the clinical activity of granulocyte-macrophage colony-stimulating factor-secreting tumor cell vaccines. *Immunol. Rev.* 222:287–298.
10. Jinushi, M., Y. Nakazaki, M. Dougan, D.R. Carrasco, M. Mihm, and G. Dranoff. 2007. MFG-E8 mediated uptake of apoptotic cells by APCs links the pro- and anti-inflammatory activities of GM-CSF. *J. Clin. Invest.* 117:1902–1913.
11. Hanayama, R., M. Tanaka, K. Miwa, A. Shinohara, A. Iwamatsu, and S. Nagata. 2002. Identification of a factor that links apoptotic cells to phagocytes. *Nature.* 417:182–187.
12. Jinushi, M., Y. Nakazaki, D.R. Carrasco, D. Draganov, N. Souders, M. Johnson, M.C. Mihm, and G. Dranoff. 2008. Milk fat globule EGF-8 promotes melanoma progression through coordinated Akt and Twist signaling in the tumor microenvironment. *Cancer Res.* 68:8889–8898.
13. Miller, A.J., and M.C. Mihm Jr. 2006. Melanoma. *N. Engl. J. Med.* 355:51–65.
14. Neutzner, M., T. Lopez, X. Feng, E.S. Bergmann-Leiner, W.W. Leiner, and M.C. Udey. 2007. MFG-E8/lactadherin promotes tumor growth in an angiogenesis-dependent transgenic mouse model of multistage carcinogenesis. *Cancer Res.* 67:6777–6785.
15. Carmon, L., I. Bobilev-Priel, B. Brenner, D. Bobilev, A. Paz, E. Bar-Haim, B. Tirosh, T. Klein, M. Fridkin, F. Lemonnier, et al. 2002. Characterization of novel breast carcinoma-associated BA46-derived peptides in HLA-A2.1/D(b)-beta2m transgenic mice. *J. Clin. Invest.* 110:453–462.
16. Meyerhardt, J. A., and R.J. Mayer. 2005. Systemic therapy for colorectal cancer. *N. Engl. J. Med.* 352:476–487.
17. Bu, H.F., X.L. Zuo, X. Wang, M.A. Ensslin, V. Koti, W. Hsueh, A.S. Raymond, B.D. Shur, and X.D. Tan. 2007. Milk fat globule-EGF factor8/lactadherin plays a crucial role in maintenance and repair of murine intestinal epithelium. *J. Clin. Invest.* 117:3673–3683.

18. Silvestre, J.S., C. Thery, G. Hamard, J. Boddaert, B. Aquilar, A. Delcayre, C. Houbron, R. Tamarat, O. Blanc-Brude, S. Heeneman, et al. 2005. Lactadherin promotes VEGF-dependent neovascularization. *Nat. Med.* 11:499–506.
19. Hanayama, R., M. Tanaka, K. Miyasaka, K. Aozasa, M. Koike, Y. Uchiyama, and S. Nagata. 2004. Autoimmune disease and impaired uptake of apoptotic cells in MFG-E8-deficient mice. *Science.* 304:1147–1150.
20. Miyasaka, K., R. Hanayama, M. Tanaka, and S. Nagata. 2004. Expression of milk fat globule epidermal growth factor 8 in immature dendritic cells for engulfment of apoptotic cells. *Eur. J. Immunol.* 34:1414–1422.
21. Kranich, J., N.J. Krautler, E. Heinen, M. Polymenidou, C. Bridel, A. Schildkecht, C. Huber, M.H. Kosco-Vibois, R. Zinkernagel, G. Miele, and A. Aquzzi. 2008. Follicular dendritic cells control engulfment of apoptotic bodies by secreting Mfge8. *J. Exp. Med.* 205:1293–1302.
22. Moore, M.W., F.R. Carbone, and M.J. Bevan. 1988. Introduction of soluble protein into the class I pathway of antigen processing and presentation. *Cell.* 54:777–785.
23. Murphy, K.M., A.B. Heimberger, and D.Y. Loh. 1990. Induction by antigen of intrathymic apoptosis of CD4+CD8+TCRlo thymocytes in vivo. *Science.* 250:1720–1723.
24. Kalergis, A.M., and J.V. Ravetch. 2002. Inducing tumor immunity through the selective engagement of activating Fcγ receptors on dendritic cells. *J. Exp. Med.* 195:1653–1659.
25. Coussens, L.M., and Z. Werb. 2002. Inflammation and cancer. *Nature.* 420:860–867.
26. Druker, B.J., and A. David. 2003. Karnofsky Award lecture. Imatinib as a paradigm of targeted therapies. *J. Clin. Oncol.* 21(23 Suppl.):239s–245s.
27. Ferrara, N. 2004. Vascular endothelial growth factor: basic science and clinical progress. *Endocr. Rev.* 25:581–611.
28. Rubin, R.H., and L.S. Young. 2002. Clinical Approach to Infection in the Compromised Host. Springer-Verlag New York Inc., New York. 100 pp.
29. Lacy-Hulbert, A., A.M. Smith, H. Tissire, M. Barry, D. Crowley, R.T. Bronson, J.T. Roes, J.S. Savill, and R.O. Hynes. 2007. Ulcerative colitis and autoimmunity induced by loss of myeloid alphav integrins. *Proc. Natl. Acad. Sci. USA.* 104:15823–15828.
30. Sosic, D., J.A. Richardson, K. Yu, D.M. Ornitz, and E.N. Olson. 2003. Twist regulates cytokine gene expression through a negative feedback loop that represses NF-kappaB activity. *Cell.* 112:169–180.
31. Dhodapkar, K.M., and M.V. Dhodapkar. 2005. Recruiting dendritic cells to improve antibody therapy of cancer. *Proc. Natl. Acad. Sci. USA.* 102:6243–6244.
32. Quezada, S.A., K.S. Peggs, M.A. Curran, and J.P. Allison. 2006. CTLA4 blockade and GM-CSF combination immunotherapy alters the intratumor balance of effector and regulatory T cells. *J. Clin. Invest.* 116:1935–1945.
33. Hodi, F.S., M. Butler, D.A. Oble, M.V. Seiden, F.G. Haluska, A. Kruse, S. Macrae, M. Nelson, C. Canning, I. Lowy, et al. 2008. Immunologic and clinical effects of antibody blockade of cytotoxic T lymphocyte-associated antigen 4 in previously vaccinated cancer patients. *Proc. Natl. Acad. Sci. USA.* 105:3005–3010.
34. Obeid, M., A. Tesniere, F. Ghiringhrlli, G.M. Fimia, L. Apetoh, J.L. Perfettini, M. Castedo, G. Miqnot, T. Panaretakis, N. Casares, et al. 2007. Calreticulin exposure dictates the immunogenicity of cancer cell death. *Nat. Med.* 13:54–61.
35. Apetoh, L., F. Ghiringhelli, A. Tesniere, M. Obeid, C. Ortiz, A. Criollo, G. Mignot, M.C. Maiuri, E. Ullrich, P. Saulnier, et al. 2007. Toll-like receptor 4-dependent contribution of the immune system to anticancer chemotherapy and radiotherapy. *Nat. Med.* 13:1050–1059.
36. Hynes, N.M., R.G. van der Most, R.A. Lake, and M.J. Smyth. 2008. Immunogenic anti-cancer chemotherapy as an emerging concept. *Curr. Opin. Immunol.* 20:545–557.
37. Gasser, S., and D.H. Raulet. 2006. The DNA damage response arouses the immune system. *Cancer Res.* 66:3959–3962.
38. Uno, T., K. Takeda, Y. Kojima, H. Yoshizawa, H. Akiba, R.S. Mittler, F. Geyjo, K. Okumura, H. Yagita, and M.J. Smyth. 2006. Eradication of established tumors in mice by a combination antibody-based therapy. *Nat. Med.* 12:693–698.
39. Johnstone, R.W., A.J. Fraw, and M.J. Smyth. 2008. The TRAIL apoptotic pathway in cancer onset, progression and therapy. *Nat. Rev. Cancer.* 8:782–798.
40. Kaiga, T., M. Sato, H. Kaneda, Y. Iwakura, T. Takayama, and H. Tahara. 2007. Systemic administration of Il-23 induces potent antitumor immunity primarily mediated through Th1-type response in association with the endogenously expressed IL-12. *J. Immunol.* 178:7571–7580.
41. Hogquist, K.A., S.C. Jameson, W.R. Heath, J.L. Howard, M.J. Bevan, and F.R. Carbone. 1994. T cell receptor antagonist peptides induce positive selection. *Cell.* 76:17–25.
42. Dranoff, G., E. Jaffee, A. Lazenby, P. Golumbek, H. Levitsky, K. Brose, V. Jackson, H. Hamada, D. Pardoll, and R.C. Mulligan. 1993. Vaccination with irradiated tumor cells engineered to secrete murine granulocyte-macrophage colony-stimulating factor stimulates potent, specific, and long-lasting anti-tumor immunity. *Proc. Natl. Acad. Sci. USA.* 90:3539–3543.

THE JOURNAL OF BIOLOGICAL CHEMISTRY VOL. 284, NO. 49, pp. 33750–33762, December 4, 2009

Non-redundant Roles of Phosphoinositide 3-Kinase Isoforms α and β in Glycoprotein VI-induced Platelet Signaling and Thrombus Formation*[S]

Received for publication, July 27, 2009, and in revised form, September 11, 2009 Published, JBC Papers in Press, October 8, 2009, DOI 10.1074/jbc.M109.048439

Karen Gilio[‡1], Imke C. A. Munnix[‡1], Pierre Mangin[§], Judith M. E. M. Cosemans[‡], Marion A. H. Feijge[‡], Paola E. J. van der Meijden[‡], Servé Olieslagers[¶], Magdalena B. Chrzanowska-Wodnicka[‖], Rivka Lillian[§], Simone Schoenwaelder[§], Shigeo Koyasu[**], Stewart O. Sage[‡‡], Shaun P. Jackson[§], and Johan W. M. Heemskerk[‡2]

From the Departments of [‡]Biochemistry and [¶]Cardiology, Cardiovascular Research Institute Maastricht, University of Maastricht, 6200 MD Maastricht, The Netherlands, the [§]Australian Centre for Blood Diseases, Monash University, Alfred Medical Research Centre and Education Precinct, Melbourne, 3800 Victoria, Australia, the [‖]Blood Research Institute, Milwaukee, Wisconsin 53233, the [**]Department of Microbiology and Immunology, Keio University School of Medicine, 160–8582 Tokyo, Japan, and the [‡‡]Department of Physiology, Development, and Neuroscience, University of Cambridge, Cambridge CB2 3EG, United Kingdom

Platelets are activated by adhesion to vascular collagen via the immunoglobulin receptor, glycoprotein VI (GPVI). This causes potent signaling toward activation of phospholipase Cγ2, which bears similarity to the signaling pathway evoked by T- and B-cell receptors. Phosphoinositide 3-kinase (PI3K) plays an important role in collagen-induced platelet activation, because this activity modulates the autocrine effects of secreted ADP. Here, we identified the PI3K isoforms directly downstream of GPVI in human and mouse platelets and determined their role in GPVI-dependent thrombus formation. The targeting of platelet PI3Kα or -β strongly and selectively suppressed GPVI-induced Ca^{2+} mobilization and inositol 1,4,5-triphosphate production, thus demonstrating enhancement of phospholipase Cγ2 by PI3Kα/β. That PI3Kα and -β have a non-redundant function in GPVI-induced platelet activation and thrombus formation was concluded from measurements of: (i) serine phosphorylation of Akt, (ii) dense granule secretion, (iii) intracellular Ca^{2+} increases and surface expression of phosphatidylserine under flow, and (iv) thrombus formation, under conditions where PI3Kα/β was blocked or p85α was deficient. In contrast, GPVI-induced platelet activation was insensitive to inhibition or deficiency of PI3Kδ or -γ. Furthermore, PI3Kα/β, but not PI3Kγ, contributed to GPVI-induced Rap1b activation and, surprisingly, also to Rap1b-independent platelet activation via GPVI. Together, these findings demonstrate that both PI3Kα and -β isoforms are required for full GPVI-dependent platelet Ca^{2+} signaling and thrombus formation, partly independently of Rap1b. This provides a new mechanistic explanation for the anti-thrombotic effect of PI3K inhibition and makes PI3Kα an interesting new target for anti-platelet therapy.

Exposed collagen in a damaged vessel wall activates platelets via their immunoglobulin family receptor, glycoprotein VI (GPVI),[3] by using a complex signal transduction pathway, which is reminiscent to the pathway employed by immune receptors in T and B cells (1, 2). In platelets, tyrosine phosphorylation of the Fc receptor γ-chain, linked to GPVI via Src family kinases, leads to a cascade of protein phosphorylation events, cumulating in the activation of phospholipase Cγ2 (PLCγ2). This key effector enzyme triggers many downstream events, including production of inositol 1,4,5-trisphosphate ($InsP_3$), mobilization of cytosolic Ca^{2+}, activation of integrin $\alpha_{IIb}\beta_3$, secretion of platelet granules loaded with autocrine-stimulating agents (ADP and ATP), and exposure of negatively charged phosphatidylserine (PS) at the platelet surface to ensure coagulation (1, 3, 4). All these responses are potently triggered by GPVI ligands, which, besides collagen, include collagen-related peptides and the snake venom convulxin (5–7).

One of the GPVI-induced signaling events contributing to PLCγ2 activation is activation of the protein/lipid kinase, phosphoinositide 3-kinase (PI3K) in both human and mouse platelets (8–11). Evidence for this role came from the finding that, in platelets stimulated with GPVI agonists, the p85α regulatory subunit of PI3K coprecipitates with the Fc receptor γ-chain and the LAT adaptor protein (8). The p85α subunit pulls p110 catalytic subunits to the membrane, where they catalyze the formation of 3-phosphorylated inositol phospholipids, primarily the phosphoinositide 3,4,5-trisphosphate ($PI(3,4,5)P_3$) (10).

Currently, there is evidence that individual class I PI3K isoforms, which are distinguished according to their catalytic subunits, have specific cellular and physiological functions. For instance, the p110α isoform (PI3Kα) has been implicated in oncogenesis, and isoform-selective PI3Kα inhibitors can reduce tumor formation (12). The p110γ isoform (PI3Kγ) is involved in innate immunity and various inflammatory diseases

* This work was supported by Grants from the EU (Marie Curie EST 2005-020706), the Netherlands Heart Foundation (2002-B014), and the Netherlands Organization for Scientific Research (NWO 11.400.0076).

[S] The on-line version of this article (available at http://www.jbc.org) contains supplemental Figs. 1 and 2 and Table I.

[1] Both authors contributed equally to this work.

[2] To whom correspondence should be addressed: Dept. of Biochemistry, Cardiology, Cardiovascular Research Institute Maastricht, University of Maastricht, P. O. Box 616, 6200 MD Maastricht, The Netherlands. Tel.: 31-43-388-1671; Fax: 31-43-388-4160; E-mail: jwm.heemskerk@bioch.unimaas.nl.

[3] The abbreviations used are: GPVI, glycoprotein VI; CRP, collagen-related peptide; $InsP_3$, inositol 1,4,5-trisphosphate; PI3K, phosphoinositide 3-kinase; $PI(3,4,5)P_3$, phosphoinositide 3,4,5-trisphosphate; PLC, phospholipase C; PPACK, H-Phe-Pro-Arg chloromethyl ketone; PRP, platelet-rich plasma; PS, phosphatidylserine; OG, Oregon Green; PH, pleckstrin homology.

(13), whereas p110δ has a more important role in adaptive immunity, *e.g.* in T and B cells (14). Human and mouse platelets contain four different PI3K isoforms, among which are the class IA catalytic subunits, p110α, -β, and -δ (PI3Kα, -β, and -δ), and the class IB catalytic subunit, p110γ (PI3Kγ) (15–17). For class IA, the corresponding regulatory subunits are p85α/β, p55α/γ, and p50α, whereas for class IB the regulatory subunit is p101γ. Structural studies in other cells have indicated that the regulatory class IA subunits, particularly p85α, can interact with tyrosine kinase-linked receptors via the SH2 domains (18). In contrast, class IB isoforms may rather interact with G-protein-coupled receptors (16). This concept was recently challenged by the observation that, in platelets, both PI3Kβ and -γ are activated via the $P2Y_{12}$ receptor for ADP, which is coupled to G_i, and that both isoforms contribute to integrin $\alpha_{IIb}\beta_3$ activation and platelet aggregation (17, 19–21). Hence, it is clear that PI3K isoforms can be activated by other platelet receptors than only GPVI.

To date, it is debated which of the PI3K isoforms become directly activated by GPVI signaling, and which are activated indirectly, *e.g.* following ADP receptor stimulation. Also unclear is which are the downstream events mediated by the various isoforms. Reasons for this lack of clarity include: (i) the large contribution to GPVI-induced responses of secondary, autocrine stimulators, particularly ADP and thromboxane (1, 17, 22); (ii) the proposed stimulation by PI3K and its product $PI(3,4,5)P_3$ to Ca^{2+} entry rather than to PLC activity (23, 24); (iii) the limited knowledge on the effector targets of PI3K and $PI(3,4,5)P_3$ in platelets, of which only phosphoinositide-dependent kinase and Akt are well studied (21, 25); (iv) the observation that p110δ is not a major isoform implicated in GPVI-induced platelet activation (26); and (v) the limited availability of mice deficient in PI3K subunits.

One possible, poorly explored target of PI3K in platelets is the small GTPase Rap1b, which is highly expressed in these cells and is considered to play a key role in the activation process particularly toward $\alpha_{IIb}\beta_3$ activation. Platelet agonists such as ADP and thrombin produce the active GTP-bound form of Rap1b, partly in a PI3K-dependent manner (27, 28). Recent findings suggest that PI3Kβ is the main isoform responsible for the ADP-induced activation of Rap1b and Akt, whereas PI3Kγ contributes to $\alpha_{IIb}\beta_3$ activation by a separate pathway (21). However, whether and how Rap1b is activated by GPVI is unresolved, as is the role of different PI3K isoforms herein.

In the present report, we studied the identity of the PI3K isoforms downstream of GPVI and determined their role in platelet activation and thrombus formation. To discriminate between direct and indirect GPVI-induced effects, the cells were stimulated in the presence of autocrine stimulation inhibitors, blocking the signaling contributions of both ADP and thromboxane. For the studies, we combined a pharmacological approach using a panel of isoform-specific PI3K inhibitors with experiments using mice deficient in distinct PI3K catalytic or regulatory subunits. We found that PI3Kα and -β are key mediators of GPVI-induced thrombus formation and show that these isoforms affect the activity of both PLCγ2 and Rap1b.

EXPERIMENTAL PROCEDURES

Mouse Strains—Mice deficient in the p85α regulatory PI3K subunit had a C57BL/6 genetic background (11, 29). Mice deficient in p110γ or p110δ (17) or deficient in Rap1b (30) were from sources previously described. All knock-out mice had normal platelet counts. Wild-type mice were used of the same background and same breeding program. Animal experiments were approved by the local animal experimental committees.

Materials—Fura-2 and Fluo-3 acetoxymethyl esters, Pluronic F-127 and Oregon Green 488-labeled fibrinogen (OG-fibrinogen) were from Molecular Probes; OG-annexin A5 was from Nexins Research; fluorescein isothiocyanate-labeled anti-human CD62 monoclonal antibody was from Sanquin. Antibodies against Akt were from Cell Signaling Technology; anti-Rap1 antibody was from BD Biosciences. LY294002 and H-Phe-Pro-Arg chloromethyl ketone (PPACK) were from Calbiochem. Wortmannin, apyrase (grade V), α-thrombin, and MRS-2179, a $P2Y_1$ antagonist, were from Sigma. Inhibitors of PI3K isoforms (supplemental Table I) and control substance PIK-112 were kind gifts from the Baker Heart Research Institute and synthesized as described (17, 31). Cangrelor (AR-C69931MX), a $P2Y_{12}$ antagonist, was kindly provided by The Medicines Co. Other reagents were from sources indicated before (32, 33).

Blood Collection and Platelet Isolation—For platelet isolation, blood was collected into one-sixth volume of acid-citrate-dextrose anticoagulant (85 mM sodium citrate, 78 mM citric acid, and 11 mM D-glucose). Donors gave full informed consent according to the Helsinki declaration and had not taken medications for 2 weeks. Platelet-rich plasma (PRP) and washed platelets were obtained by centrifugation, as described for human (7) and mouse (32, 33) platelets. Washed human platelets were resuspended in Hepes buffer, pH 7.45 (137 mM NaCl, 10 mM Hepes, 2.7 mM KCl, 2 mM $MgSO_4$, 0.42 mM D-glucose, 0.2 unit/ml apyrase, and 0.1% bovine serum albumin, pH 7.45). Mouse platelets were resuspended in a modified Hepes buffer (33). Platelets were counted with a Coulter counter. For whole blood flow experiments, human blood was collected into 40 μM PPACK (34), whereas mouse blood was collected into 40 μM PPACK plus 5 units/ml heparin (32).

Intracellular Ca^{2+} Measurement in Platelet Suspensions—Human PRP (2×10^8 platelets/ml) was loaded with 2.5 μM Fura-2 acetoxymethyl ester in the presence of aspirin (100 μM) and apyrase (0.2 unit of ADPase/ml) at 37 °C for 45 min (35). The loaded platelets were resuspended in Hepes buffer, pH 7.45 (1×10^8/ml), and were used within 90 min. Before addition of agonist, the cells were preincubated with apyrase (0.1 unit/ml) and ADP receptor blockers (40 μM MRS-2179 for $P2Y_1$ and 10 μM ARC-69931MX for $P2Y_{12}$) to inhibit autocrine stimulation. In some experiments, apyrase was added at a high concentration (0.6 unit/ml). Platelet preincubation with indicated PI3K inhibitors or Me_2SO vehicle was for 10 min (37 °C). Calcium responses were recorded under stirring with an SLM-Aminco or a Cairn Research spectrofluorometer, at alternate excitation wavelengths of 340 and 380 nm (37 °C). The 340/380 nm ratio values were converted into nanomolar concentrations of $[Ca^{2+}]_i$, as described (35). Separate calibrations were done for

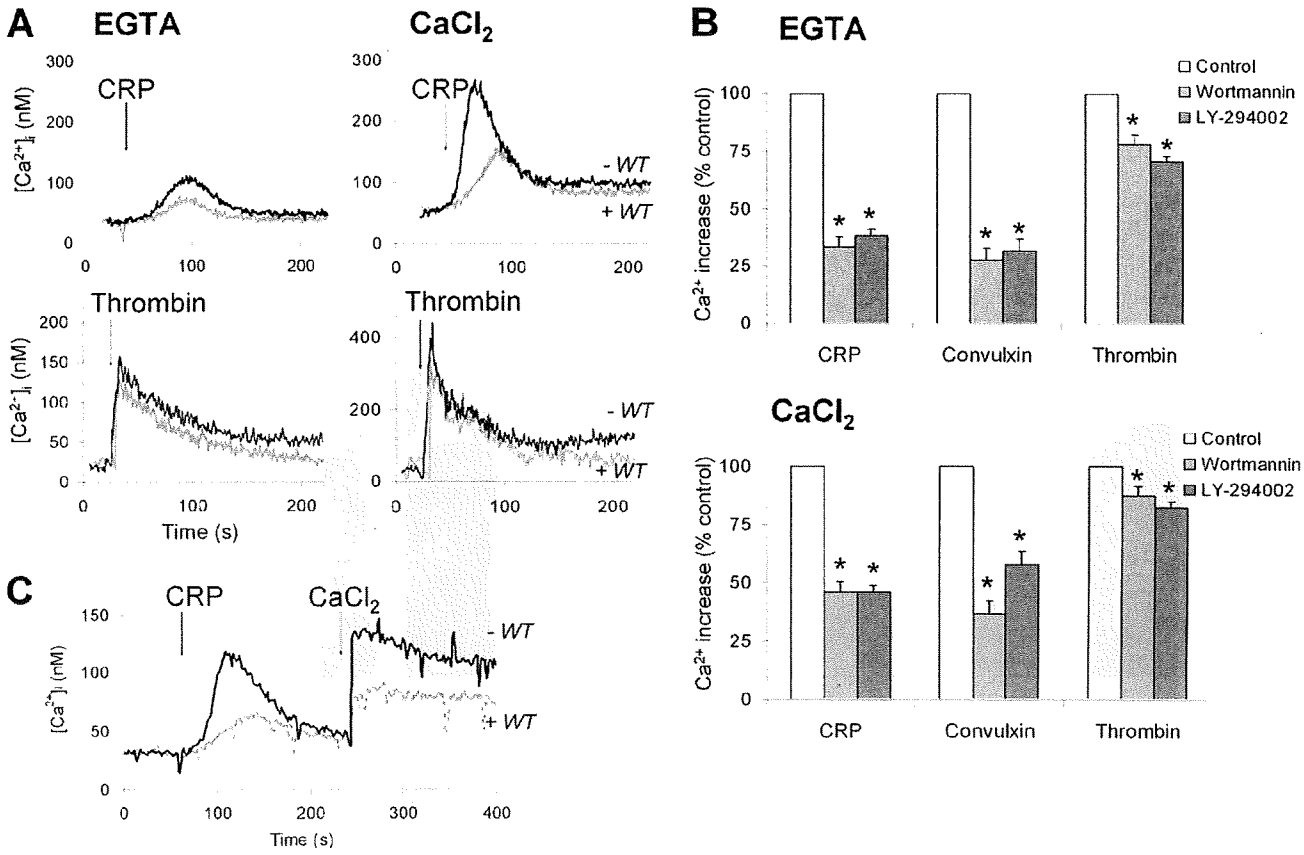

FIGURE 1. **Major contribution of PI3K to GPVI-induced *versus* thrombin receptor-induced Ca^{2+} responses in absence of autocrine mediators.** Human platelets, treated with aspirin and loaded with Fura-2, were preincubated for 10 min with Me_2SO vehicle (*control*), wortmannin (0.1 μM), or LY-294002 (10 μM) in the presence of apyrase (0.6 unit/ml). The platelets were stimulated with GPVI ligand, CRP (5 μg/ml), or convulxin (70 ng/ml), or with thrombin (10 nM), in the presence of 1 mM EGTA or 1 mM $CaCl_2$. *A*, effect of wortmannin (*WT*) on CRP-induced $[Ca^{2+}]_i$ increases. *B*, quantitative effect of wortmannin and LY-294002 on integrated Ca^{2+} responses in the presence of EGTA or $CaCl_2$. Per agonist, time-$[Ca^{2+}]_i$ integrals of the relevant control condition were set at 100%. *C*, effect of wortmannin on convulxin-induced Ca^{2+} mobilization and secondary Ca^{2+} entry (1 mM $CaCl_2$). Representative traces are shown. Means ± S.E. ($n = 4–5$); *, $p <$ 0.05 compared with control.

incubations containing colored PI3K inhibitors. Rises in $[Ca^{2+}]_i$ were expressed as 5-min time integrals, to quantify prolonged Ca^{2+}-signaling effects (36).

Platelet Aggregation and Flow Cytometry—Human PRP was pretreated with aspirin, and platelets were washed. The washed platelets were preincubated for 10 min with autocrine stimulation inhibitors (see above) and PI3K blockers or Me_2SO vehicle. After 10 min of activation, samples were analyzed by flow cytometry for P-selectin expression using fluorescein isothiocyanate-anti-CD62 monoclonal antibody (1:100) or for $\alpha_{IIb}\beta_3$ activation using fluorescein isothiocyanate-labeled PAC1 monoclonal antibody (37).

Washed mouse platelets were prepared from PRP (21) and preincubated with a mixture of autocrine stimulation inhibitors (100 μM MRS-2179, 10 μM AR-C69931MX, and 10 μM indomethacin). Platelet aggregation was measured, as described (21). OG488-fibrinogen binding to the platelets was assessed by flow cytometry (33).

InsP Measurement—Accumulation of $InsP_1$ due to $InsP_3$ production was measured with an IP-One ELISA kit from Cis-Bio, determining $InsP_1$ levels. Aspirin-treated platelets (1×10^8/ml) were preincubated with ADP receptor blockers, LiCl (1 mM), and Me_2SO vehicle or PI3K blocker. After stimulation for 5–10 min with convulxin or thrombin, the platelets were lysed. Cell lysates were incubated with $InsP_1$-horseradish peroxidase conjugate and anti-$InsP_1$ monoclonal antibody, according to the manufacturer's instructions.

Activation of Akt and Rap1 by Western Blotting—Akt activation was measured by Western blot analysis of platelet lysates. A polyclonal anti-phosphoserine-473 Akt antibody was used to detect active Akt and a polyclonal anti-Akt antibody to determine total Akt (19). Activation of Rap1 was measured in platelet lysates by selective precipitation of GTP-bound Rap1 using glutathione *S*-transferase-RalGDS bound to glutathione-Sepharose (28). Western blotting was performed with anti-Rap1 antibody (250 ng/ml) and a sheep anti-mouse horseradish peroxidase-coupled secondary antibody (1:5000).

Thrombus Formation and Procoagulant Activity under Flow—Perfusion of PPACK-anti-coagulated human blood (34) and of PPACK/heparin-anti-coagulated mouse blood (32) was done in the absence of coagulation as described. Blood samples were preincubated with PI3K inhibitor or Me_2SO vehicle for 10 min. Blood was flowed through a transparent, parallel-plate flow chamber, containing a collagen-coated coverslip, at a defined

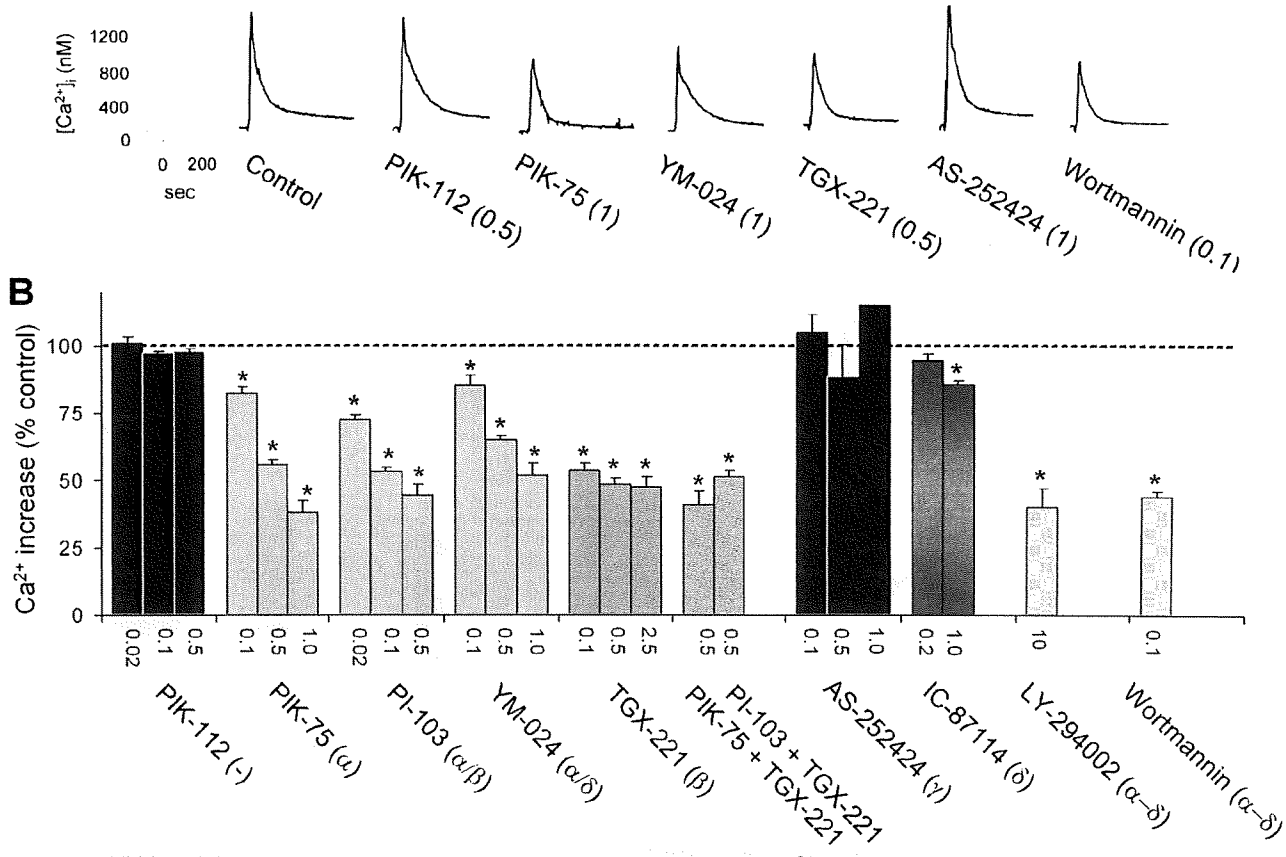

FIGURE 2. **Inhibition of platelet PI3Kα and -β isoforms strongly suppresses GPVI-induced Ca^{2+} responses.** Aspirin-treated, Fura-2-loaded platelets were preincubated with ADP receptor blockers (10 μM AR-C69931MX, 40 μM MRS-2179, and 0.1 unit/ml apyrase) and 1 mM $CaCl_2$. Platelets were then treated with one of the following substances (PI3K isoform specificity in *parentheses*): Me_2SO vehicle (*control*), PIK-112 (inactive analog of PIK-75), PIK-75 (α), PI-103 (α/β), YM-024 (α/δ), TGX-221 (β), AS-252424 (γ), IC-87114 (δ), LY-294002 (α through δ), or wortmannin (α through δ). *Numbers* give final concentrations in micromolar. *A*, representative $[Ca^{2+}]_i$ traces upon stimulation with convulxin (70 ng/ml). *B*, effects of inhibitors on Ca^{2+} responses, expressed as percentages of time-$[Ca^{2+}]_i$ integrals relative to the control condition. Note that at a low dose of convulxin (7 ng/ml), PIK-75, TGX-221, or the combination of both (0.5 μM) suppressed the Ca^{2+} rise to 51 ± 3%, 40 ± 6%, or 31 ± 1% of control, respectively. Data are means ± S.E. (n = 3–5); *, $p < 0.05$ compared with control.

shear rate for 4 min. The thrombi in flow chambers were stained by rinse with Hepes buffer, pH 7.45, supplemented with 1 unit/ml heparin, 2 mM $CaCl_2$, and OG488-annexin A5 (1 μg/ml). Microscopic images were recorded in real-time using a Visitech imaging system, equipped with two intensified charge-coupled device cameras (34). Bright-field contrast and fluorescence digital images were taken from >10 randomly chosen fields. ImagePro software (Media Cybernetics) was used to quantify platelet deposition (38).

Intracellular Ca^{2+} Measurement under Flow—Human PRP (2×10^8/ml) was incubated with 7 μM Fluo-3 acetoxymethyl ester for 45 min at 20 °C under gentle rotation. Washed mouse platelets (2×10^8/ml) were incubated with 5 μM Fluo-3 acetoxymethyl ester plus 0.2 mg/ml Pluronic F-127. The dye-loaded cells were added to autologous blood (10% labeled platelets) and used for flow experiments within 1 h. Fluorescence images were recorded during high speed (5 Hz) perfusion of blood over a collagen surface (39). Off-line, regions of interest representing one adhered cell were analyzed for fluorescence changes. Raw fluorescence data were converted into F/F_0 values by pseudo-ratio analysis, and then into nanomolar concentrations of $[Ca^{2+}]_i$ (40). For quantification, traces from individual cells were superimposed, so that frame numbers of initial $[Ca^{2+}]_i$ increases coincided.

Statistics—Differences between groups were tested with a Mann-Whitney U test or analysis of variance. Effects of inhibitors were tested with a Student's paired t test. The statistical package for social sciences was used (SPSS 15.0).

RESULTS

Prominent Roles of PI3Kα and -β Isoforms in GPVI-induced Ca^{2+} Responses—Although PI3K activity has been implicated in GPVI-mediated platelet activation, it is unclear whether its role is direct or indirect, *e.g.* via autocrine ADP release and $P2Y_{12}$ signaling. Another proposal is that PI3K may specifically stimulate GPVI-induced Ca^{2+} entry rather than mobilization of Ca^{2+} from internal stores (23). To investigate this further, human Fura-2-loaded platelets were activated with GPVI agonist under conditions where indirect effects of autocrine stimulators (thromboxane A_2 and ADP) were prevented with aspi-

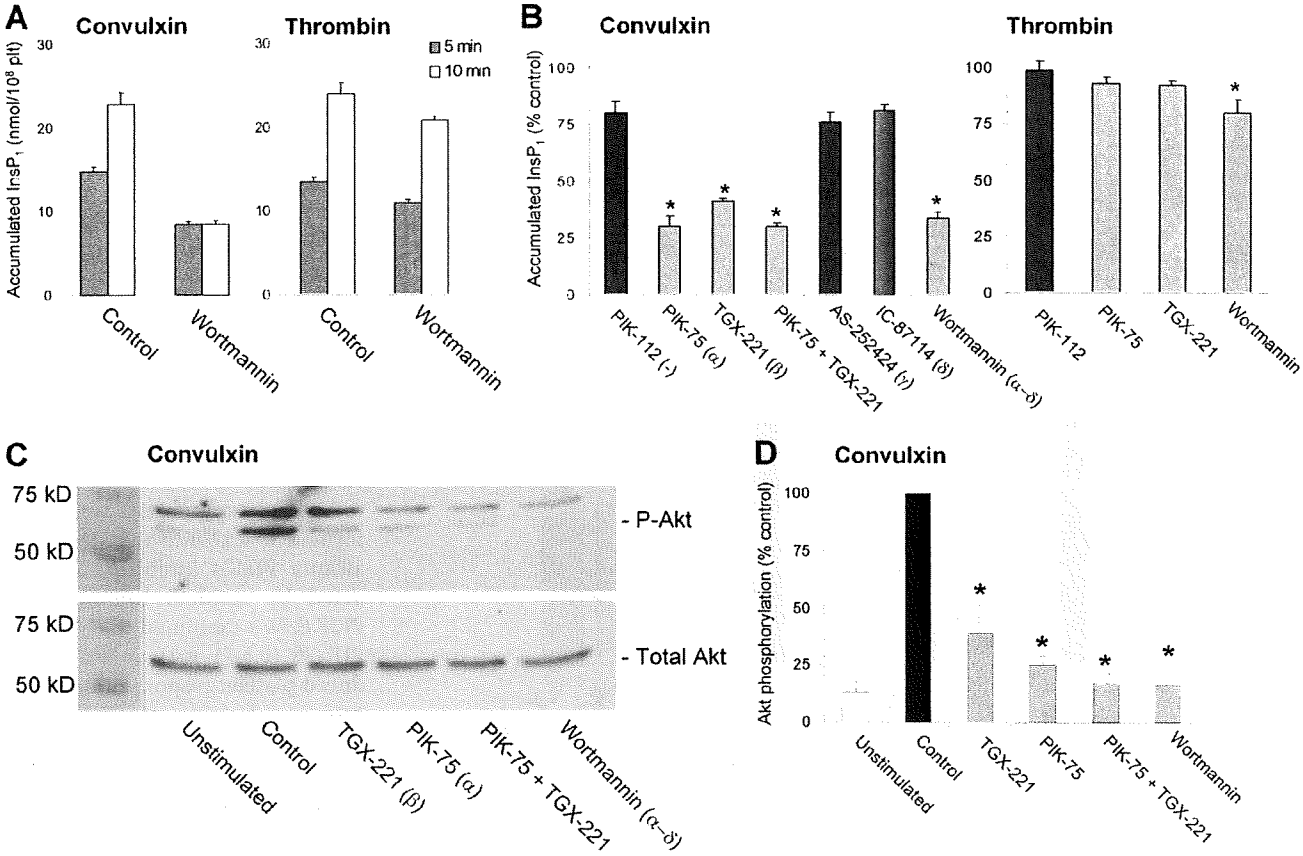

FIGURE 3. **Contribution of PI3Kα and -β isoforms to GPVI-induced $InsP_3$ production and Akt phosphorylation.** Aspirin-treated human platelets (1×10^8/ml) were preincubated with ADP receptor blockers (Fig. 2) and Me_2SO vehicle (control) or 1 μM PI3K inhibitor (25 μM LY-294002). *A* and *B*, effect of PI3K blockers on accumulation of $InsP_1$ due to $InsP_3$ production. Platelets were stimulated for 10 min with convulxin (70 ng/ml) or thrombin (10 nM) in the presence of 1 mM LiCl. *C* and *D*, effect of PI3K blockers on convulxin-induced Ser^{473} Akt phosphorylation. *C*, representative Western blots of phospho-Akt and total Akt (60 kDa). *D*, data are densitometric intensities of phospho-Akt/Akt, expressed as percentage of vehicle. Means ± S.E. (n = 3–5); *, $p < 0.05$ compared with PIK-112 or control.

rin and a high concentration of ADP-degrading apyrase (0.6 unit/ml). When platelets were stimulated with CRP in the presence of extracellular EGTA (where Ca^{2+} is only mobilized from internal stores), the general PI3K inhibitor wortmannin (0.1 μM) caused ~60% suppression of the Ca^{2+} signal (Fig. 1*A*). In the presence of extracellular $CaCl_2$ (where Ca^{2+} entry takes place in addition), wortmannin had a similar inhibitory effect on the Ca^{2+} signal. The treatment of platelets with another general PI3K inhibitor, LY-294002 (25 μM), was as effective as wortmannin. Furthermore, similar effects were obtained with both inhibitors, when platelets were stimulated with the GPVI ligand, convulxin (Fig. 1*B*). To directly determine the inhibitor effect on Ca^{2+} entry, platelets were first stimulated with GPVI ligand causing Ca^{2+} mobilization, after which $CaCl_2$ was added and Ca^{2+} entry was allowed. Strikingly, wortmannin suppressed both parts of the Ca^{2+} signal at similar extent (Fig. 1*C*). A control experiment indicated that blocking anti-GPIb antibodies did not affect the convulxin-induced Ca^{2+} response (not shown), thus excluding involvement of GPIb-induced Ca^{2+} signal generation with this agonist.

Interestingly, treatment of the platelets with wortmannin or LY-294002 caused only small inhibition of the thrombin-evoked Ca^{2+} responses in both EGTA and $CaCl_2$ medium (Fig. 1*B*). Together, these data suggest that PI3K activity primarily enhances PLCγ2-evoked Ca^{2+} mobilization from stores, whereas it only secondarily affects Ca^{2+} entry.

Various new isoform-specific catalytic site inhibitors of class I PI3Ks have been developed and used for functional studies in other cell types (31, 41). The selectivity of these inhibitors for PI3Kα through δ isoforms is mostly determined in cell-free *in vitro* studies using isolated enzymes (IC_{50} values are given in supplemental Table I). The compound PIK-75 has a far higher affinity for PI3Kα (IC_{50} 8 nM) than for other isoforms. At nanomolar concentrations, the compound PI-103 inhibits both PI3Kα and -β (PIK-112 is an inactive analog). YM-024 has a relatively high affinity for PI3Kα and -δ, whereas TGX-211 is most active against PI3Kβ (IC_{50} 7 nM). The compounds AS-252424 and IC-87114 show highest activity toward PI3Kγ and PI3Kδ isoforms, respectively. It should be remarked that effective doses of these compounds for complete inhibition of the kinase activity in adipocytes, hepatoma cell lines, and platelets are reported to be in the low micromolar range (17, 21, 41). Hence, for adequate inhibition of PI3K activities in intact platelets, higher doses are needed than apparent from the IC_{50} values. Reasons for this are the high platelet counts

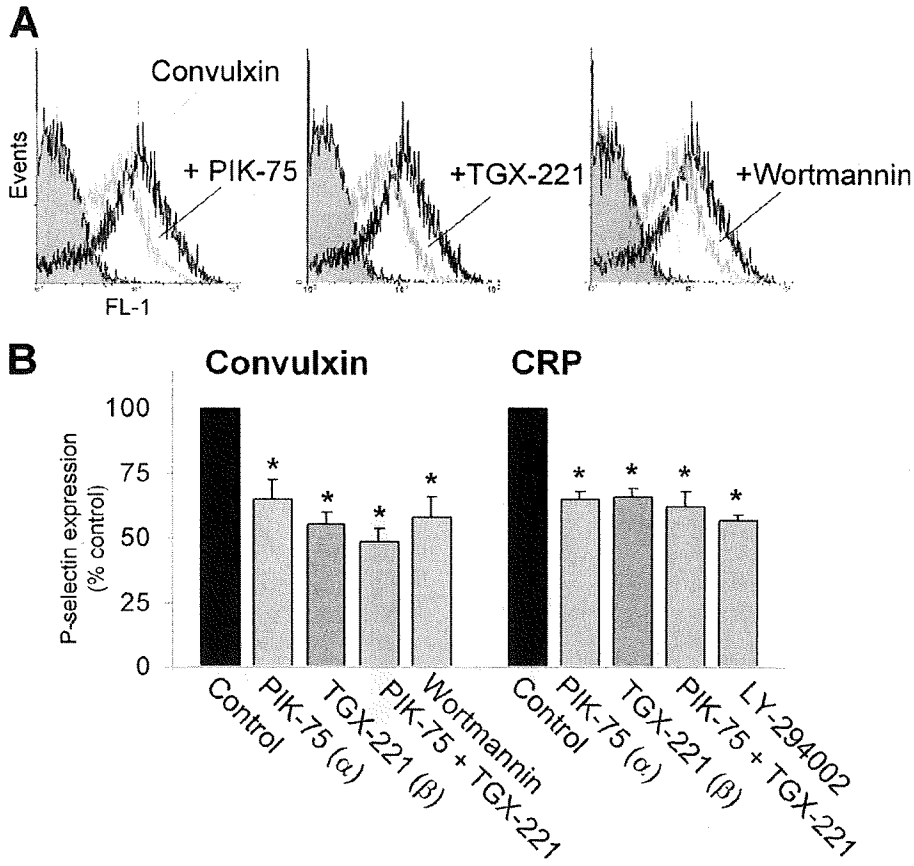

FIGURE 4. **Contribution of PI3Kα and -β isoforms to GPVI-induced α-granule secretion.** Human washed aspirin-treated platelets (1×10^8/ml) were preincubated with ADP receptor blockers (Fig. 2) and treated with Me_2SO vehicle (*control*) or specific PI3K inhibitor (in micromolar): PIK-75 (1.0), TGX-221 (0.5), wortmannin (0.1), and LY-294002 (25). The platelets were activated for 10 min with convulxin (70 ng/ml) or CRP (10 μg/ml). *A*, histogram showing effect of PI3Kα/β blockers on P-selectin expression (FL1 fluorescence). *B*, quantitative effect of PI3K blockage on P-selectin expression. Data are relative to the control condition. Means ± S.E. ($n = 3$); *, $p < 0.05$ compared with control.

in experiments and the high ATP concentration in cells (at least 10-fold higher than of *in vitro* kinase assays).

For the above-mentioned inhibitors, dose-effect relations were determined for convulxin-induced Ca^{2+} responses in $CaCl_2$ medium. To prevent autocrine stimulatory effects of thromboxane and ADP, all experiments were carried out with aspirin-treated platelets, and blockers of both ADP receptors were added. Time integrals of increases in $[Ca^{2+}]_i$ served as a read-out of the extent of GPVI-induced PLC activation (36). Strikingly, those inhibitors with a high affinity toward PI3Kα (PIK-75, PI-103, and YM-024, 0.5–1 μM) reduced the Ca^{2+} signal with ~50%, whereas the control substance PIK-112 was completely inactive (Fig. 2, *A* and *B*). In addition, the PI3Kβ selective inhibitor TGX-221 (0.1–2.5 μM) caused a similar reduction in Ca^{2+} signal. Combined application of PIK-75/TGX-221 or PI-103/TGX-221 did not further suppress the response. In general, the isoform-specific PI3Kα or -β inhibitors were similarly effective as the general PI3K inhibitors, wortmannin and LY-294002. On the other hand, AS-252424 (0.1–1 μM), inhibiting PI3Kγ, was without any effect, whereas the PI3Kδ inhibitor IC-87114 only slightly reduced the Ca^{2+} response.

For comparison, the same panel of inhibitors was tested in measurements of thrombin-induced Ca^{2+} responses. Here, only compounds with a high affinity toward PI3Kβ (*i.e.* PI-103 and TGX-221) and the general PI3K inhibitors (wortmannin and LY-294002) reduced the Ca^{2+} signal by 15–20% (supplemental Fig. 1). In this case, the PI3Kα inhibitor PIK-75 was without effect. Together, these results point to high and non-redundant roles of the PI3Kα and -β isoforms in Ca^{2+} signaling directly downstream of GPVI, but not of thrombin receptors.

Control experiments were performed to exclude that the high affinity PI3Kα inhibitor, PIK-75, acted by residual inhibition of PI3Kβ. We examined the effect of PIK-75 (0.5–1 μM) on $P2Y_{12}$-induced platelet responses and integrin $\alpha_{IIb}\beta_3$ activation, because these are exclusively mediated by the PI3Kβ and -γ isoforms (20, 21). As shown in supplemental Fig. 2, PIK-75 was completely inactive in both platelet aggregation and integrin activation in response to ADP, in marked contrast to the established PI3Kβ inhibitor, TGX-221. On the other hand, TGX-221 did not affect Akt phosphorylation at Ser^{473} evoked by insulin-like growth factor-1, which is known to be mediated by only the PI3Kα isoform (S. Kim, data not shown, but see Ref. 42).

Contribution of Both PI3Kα and -β Isoforms to GPVI-induced Signaling—In platelets, the GPVI receptor activates the PH-domain containing PLCγ2, in contrast to thrombin receptors, which activate PLCβ isoforms. For other cells, it was hypothesized that an increase in $PI(3,4,5)P_3$ level caused by PI3K pulls PLCγ2 to the membrane and increases its action (18). To verify this for GPVI-stimulated platelets (again with blocked autocrine responses), we determined overall PLC activity by measuring the accumulation of $InsP_1$ due to $InsP_3$ production. Platelet stimulation with convulxin led to a production of $InsP_3$ for up to 10 min (Fig. 3*A*). Wortmannin treatment reduced the $InsP_3$ formation and moreover confined it to 5 min. Such a shortening of $InsP_3$ production was not seen in thrombin-stimulated platelets. The isoform-specific inhibitors, PIK-75 or TGX-221 (targeting at PI3Kα and -β, respectively) suppressed the $InsP_3$ production to a similar extent as wortmannin, whereas the combination of the two did not have an additional effect (Fig. 3*B*). In contrast, inhibition of PI3Kγ (AS-252424) or PI3Kδ (IC-87114) was

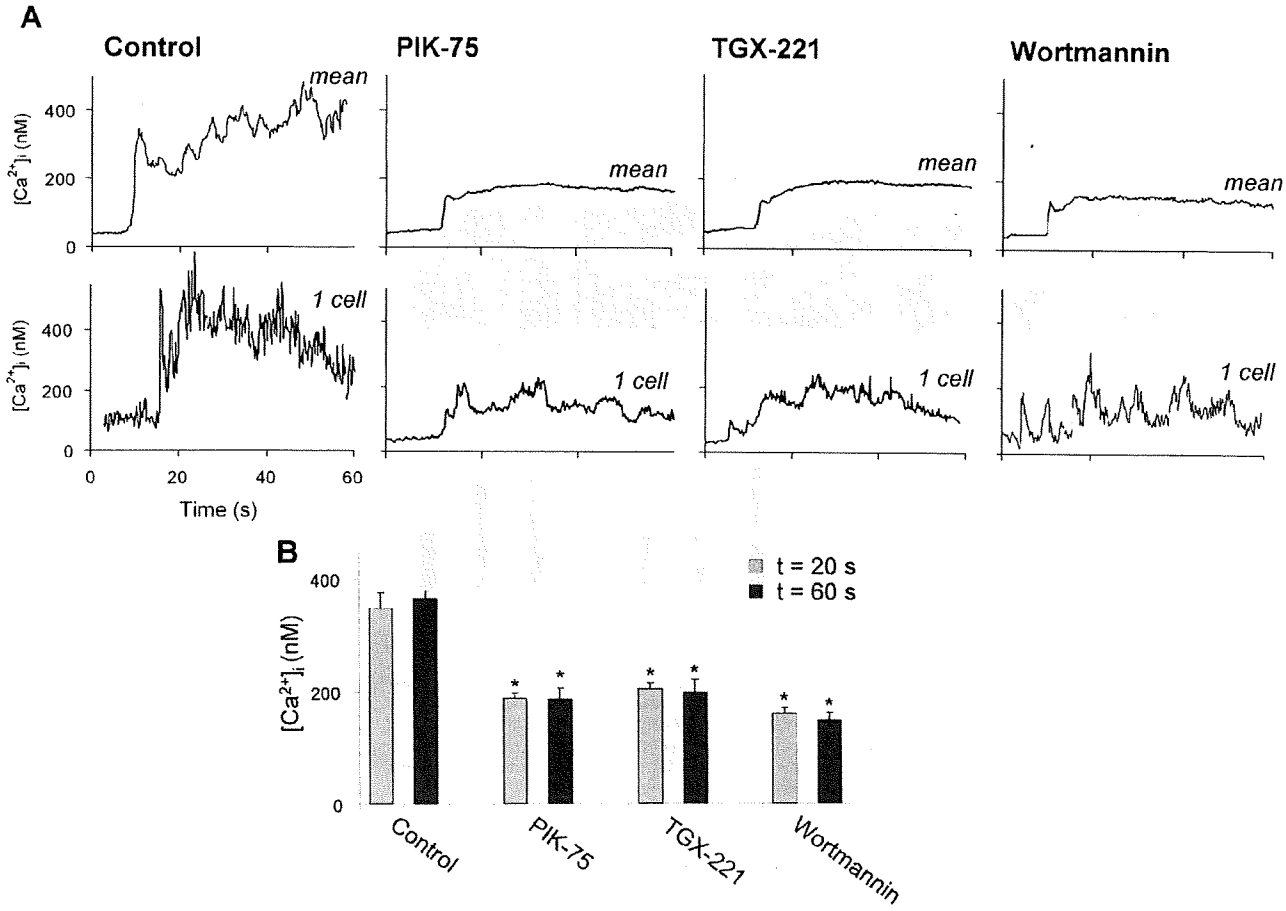

FIGURE 5. **Role of PI3K in collagen-induced Ca^{2+} responses under flow in the absence of secondary mediators.** PPACK-anti-coagulated blood, containing 10% autologous Fluo-3-loaded platelets, was preincubated with Me_2SO vehicle (*control*), PIK-75, TGX-221, or wortmannin (each 1 μM). *A*, single cell Ca^{2+} responses during flow of blood over collagen in the presence of indicated inhibitor at a shear rate of 1000 s^{-1}. *Upper panels*: mean overlays of $[Ca^{2+}]_i$ traces from >27 individual platelets; *lower panels*: traces from representative single platelets. *B*, quantification of increases in $[Ca^{2+}]_i$ at 20 s (*gray*) or 60 s (*dark gray*) after initial platelet activation. Means ± S.E. (n = 27–50); *, $p < 0.05$ compared with control.

not effective on $InsP_3$ amounts. Hence, these results point to a GPVI-induced prolongation of PLC activity by PI3Kα/β.

We measured agonist-induced Ser^{473} phosphorylation of Akt as an established downstream effector of lipid PI3K (21). In platelets stimulated with convulxin (Fig. 3*C*) or CRP (not shown), wortmannin treatment suppressed the phosphorylation of Akt, as expected. Interestingly, also inhibition of PI3Kα (PIK-75) or -β (TGX-221) reduced this phosphorylation, whereas the combination was not more effective (Fig. 3*D*).

A key downstream effect of $[Ca^{2+}]_i$ elevation in platelets is the secretion of α-granules, which is measured as expression of granular P-selectin at the platelet surface. Platelet treatment with PIK-75 or TGX-221, alone or in combination, suppressed convulxin- or CRP-induced P-selectin expression with 40–50%, *i.e.* to the same extent as did wortmannin or LY-294002 (Fig. 4). This points to a non-additive effect of both isoform-selective compounds on GPVI-induced secretion.

Roles of PI3Kα and -β Isoforms in GPVI-induced Platelet Activation and Thrombus Formation on Collagen under Flow—The pharmacological evidence so far points to a common role of the PI3Kα/β isoforms in GPVI-induced Ca^{2+} signaling and downstream platelet activation events. We then performed studies to determine the importance of these isoforms in flow-dependent thrombus formation at physiological shear rates. Earlier work has shown that, during platelet interaction with collagen under flow, GPVI-induced increases in $[Ca^{2+}]_i$ are important for granule secretion, activation of integrins, and exposure of PS (22, 34, 43, 44). In whole blood, supplemented with Fluo-3-loaded platelets, $[Ca^{2+}]_i$ increases were measured of individual platelets upon adhesion to collagen under flow. Interestingly, pretreatment with either PIK-75, TGX-221, or wortmannin led to a marked suppression in single cell Ca^{2+} responses, so that the adhered platelets showed low amplitude spiking changes in $[Ca^{2+}]_i$ (Fig. 5). Control experiments indicated that the Ca^{2+} responses under flow were not influenced by aspirin and blockage of ADP receptors (not shown), thus confirming that autocrine ADP release did not contribute to this initial platelet response. Other controls indicated that these $[Ca^{2+}]_i$ increases were completely suppressed by blocking GPVI (22).

The effects of inhibitors on thrombus formation were assessed from measurements of the deposition of platelets on the collagen surface (Fig. 6*A*). In addition, the exposure of PS of collagen-adhered platelets (detected with OG-annexin A5) was

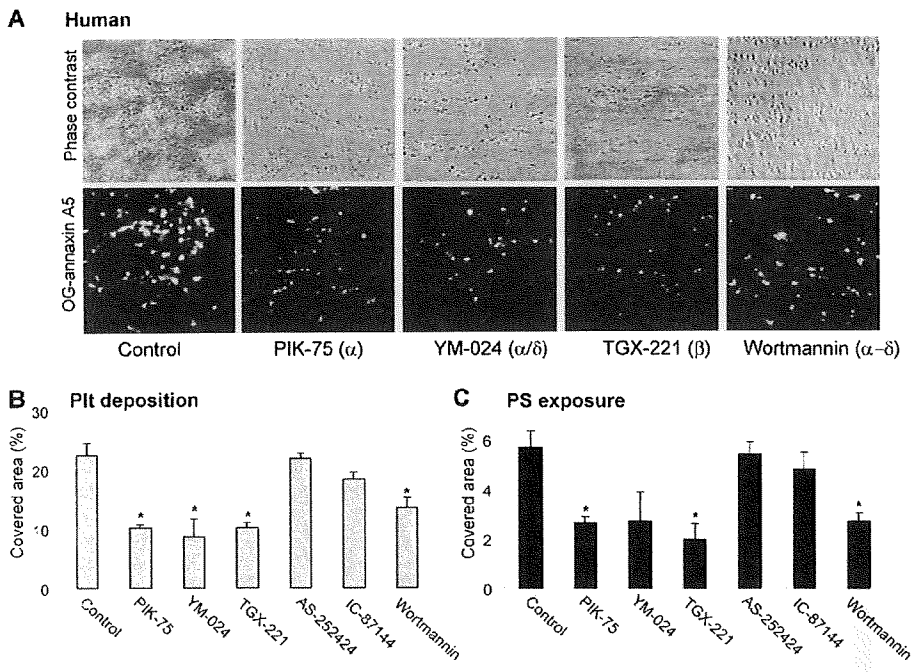

FIGURE 6. **Role of PI3Kα and -β isoforms in collagen-induced thrombus formation and PS exposure under flow.** PPACK-anti-coagulated blood was flowed during 4 min over collagen at a shear rate of 1000 s^{-1}. Preincubation was with Me_2SO vehicle (*control*) or one of the PI3K inhibitors: PIK-75, YM-024, TGX-221, AS-252424, IC-87144, or wortmannin (all 1 μM). *A*, representative images of phase contrast (120 × 120 μm) and OG-annexin A5 fluorescence (150 × 150 μm) after 4-min flow. *B* and *C*, surface area coverage of all deposited platelets and PS-exposing platelets. Data are expressed as percentages of control condition. Means ± S.E. (n = 4); *, $p < 0.05$ compared with control.

measured, the response for which is shown by a subpopulation of the platelets in direct contact with collagen due to GPVI activation (38). Both parameters were substantially diminished with wortmannin, with the PI3Kα inhibitors PIK-75 and YM-024, or with the PI3Kβ inhibitor TGX-221. In the presence of all inhibitors, platelet deposition on collagen was substantially reduced in comparison to the vehicle control (Fig. 6*B*). In addition, the number of PS-exposing platelets was reduced to ~50% by PIK-75, YM-024, or TGX-221. On the other hand, inhibition of PI3Kγ (AS-252424) or -δ (IC-87114) was without effect. Together, these results suggest that inhibition of only PI3Kα or -β isoforms suppresses flow-dependent thrombus formation on collagen, by reducing GPVI-dependent Ca^{2+} responses and downstream activation processes leading to platelet aggregation and PS exposure.

Roles of Murine PI3K Isoforms in GPVI-induced Platelet Activation and Thrombus Formation—Platelets from mice lacking the p85α regulatory PI3K subunit are impaired in collagen-induced aggregation, which points to diminished GPVI signaling (11). In the $p85\alpha^{-/-}$ platelets, expression of the p110α subunit (PI3Kα) is almost undetectable, while both p85β and p110β are still present at low levels (11, 29, 45). We used blood from $p85\alpha^{-/-}$ mice to measure collagen-dependent $[Ca^{2+}]_i$ increases in adhered platelets, thrombus formation, and PS exposure under flow. In contrast to the potent and prolonged Ca^{2+} responses of $p85\alpha^{+/+}$ platelets, $p85\alpha$-deficient platelets showed a markedly lower Ca^{2+} signal, which in 36% of the cells showed spiking Ca^{2+} responses (Fig. 7*A*). Treatment of $p85\alpha^{+/+}$ blood with TGX-221 reduced the average Ca^{2+} signal to the level seen in $p85\alpha^{-/-}$ platelets. Treatment of wild-type blood with YM-024 had a similar suppressive effect on the Ca^{2+} response (p = 0.012). As a comparison, blood was used from $p110\gamma^{-/-}$ mice, in which case Ca^{2+} responses under flow were not different from those of corresponding wild-type platelets.[4]

Measurements of flow-dependent thrombus formation on collagen showed a reduced deposition of $p85\alpha^{-/-}$ platelets, as well as a reduced PS exposure of the cells in comparison to wild-type blood (Fig. 7*B*). Similarly, addition of TGX-221 to $p85\alpha^{+/+}$ blood, but not to $p85\alpha^{-/-}$ blood, significantly decreased thrombus formation and number of PS-exposing platelets. A role for PI3Kα and -β in murine thrombus formation was further supported by inhibitor studies using blood from wild-type mice. Treatment with PIK-75 and/or TGX-221 led to a similar reduction in platelet deposition and PS exposure as treatment with the general PI3K inhibitor, wortmannin (Fig. 7*C*). Together, these results demonstrated that, in mouse, the regulatory p85α subunit and the catalytic PI3Kα and -β subunits are essential in flow-dependent Ca^{2+} signaling, PS exposure, and thrombus formation on collagen.

Experiments carried out with washed mouse platelets, in the presence of autocrine stimulation inhibitors, confirmed that GPVI-induced activation relied on PI3Kα/β activity, because LY-294002, PIK-75, and TGX-221 all inhibited CRP-induced aggregation (not shown). In addition, platelets from mice lacking the catalytic p110γ or p110δ subunits were essentially unaltered in aggregation, when compared with wild-type platelets.[5] Together, this points to major functions of murine p110α and p110β PI3K isoforms and to minor roles for p110γ and p110δ in the aggregation response.

Roles of PI3K Isoforms in GPVI-induced Rap1b Activation in Human and Mouse Platelets—In platelets, the low molecular weight GTPase, Rap1b, is a well characterized effector downstream of PI3K (27). However, there is no conclusive evidence how Rap1b functions directly downstream of GPVI. Platelets from mice deficient in Rap1b were used to investigate this. In the presence of autocrine stimulation inhibitors, $Rap1b^{-/-}$ platelets showed a 36% reduction in CRP-induced aggregation in comparison to $Rap1b^{+/+}$ wild types (Fig. 8, *A* and *B*). This suggested a direct role for this GTPase in GPVI-induced platelet aggregation. Inhibition of PI3K with LY-294002 markedly

[4] I. Munnix, unpublished data.
[5] P. Mangin, unpublished data.

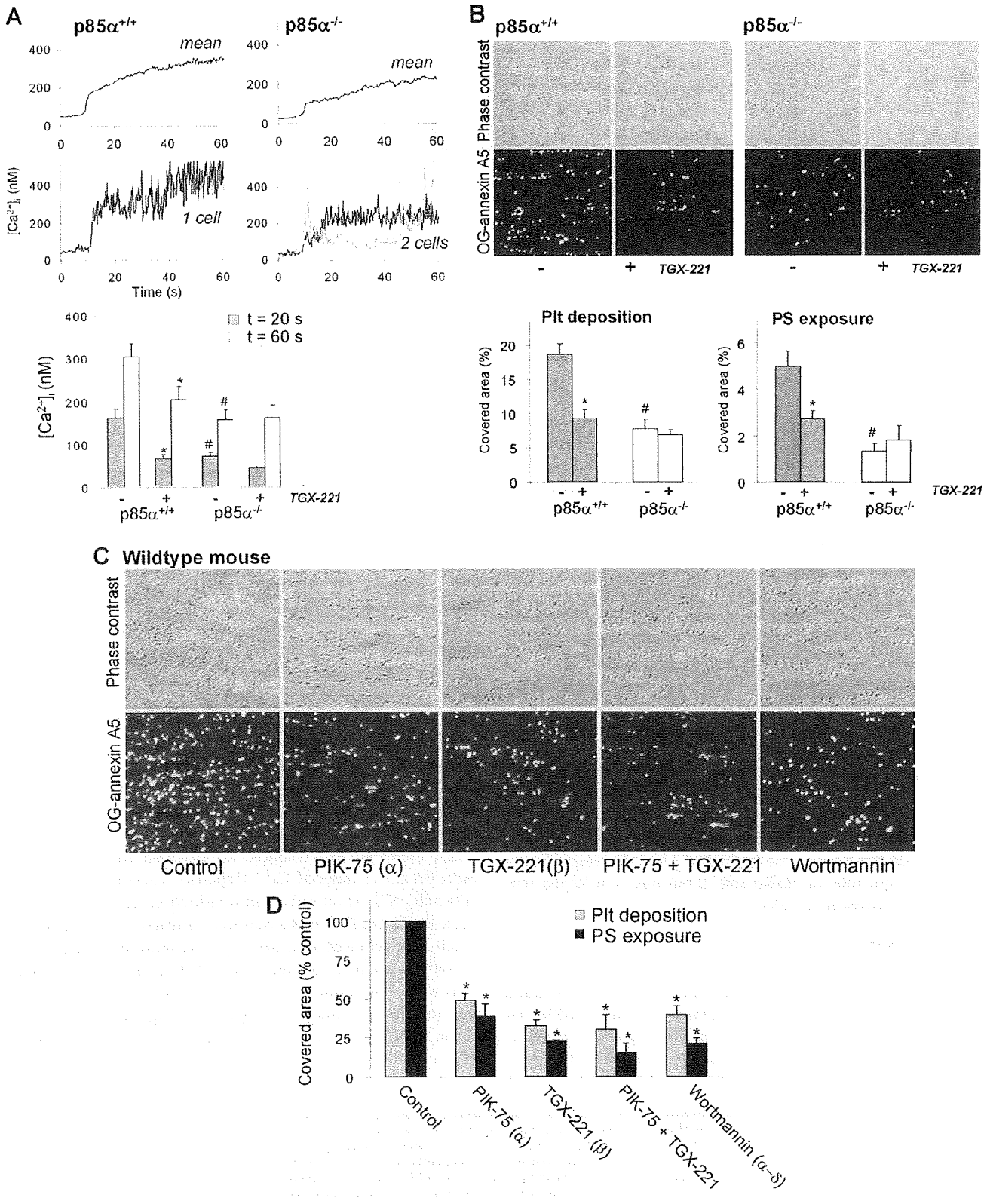

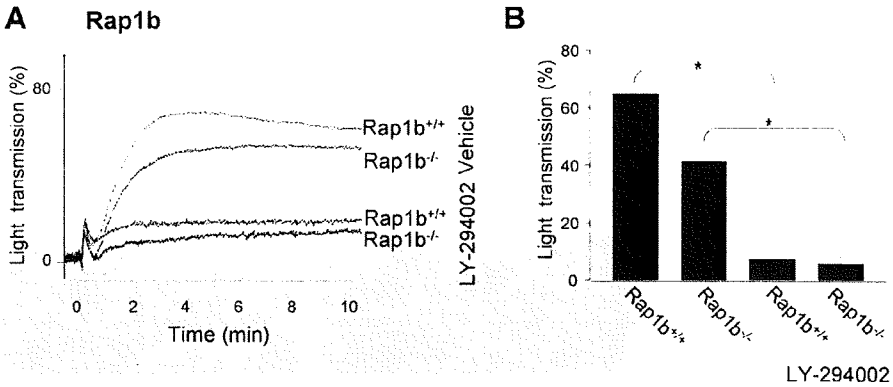

FIGURE 8. **Contribution of Rap1b to GPVI-induced integrin $\alpha_{IIb}\beta_3$ activation and platelet aggregation.** *A*, washed platelets (3×10^8/ml) from *Rap1b*$^{+/+}$ or *Rap1b*$^{-/-}$ mice were preincubated with autocrine stimulation inhibitors (AR-C69931MX, MRS-2179, and 10 μM indomethacin), in the presence of Me_2SO vehicle or LY-294002 (25 μM). Platelets were stimulated with 10 μg/ml CRP in the presence of purified fibrinogen (0.5 mg/ml), and aggregation was monitored. Representative aggregation traces are shown. *B*, *bars* give percentages of light transmission at 3 min after CRP addition. Data are means ± S.E. ($n = 3$–4); *, $p < 0.05$ compared with control.

reduced the aggregation of *Rap1b*$^{+/+}$ platelets and, surprisingly, of *Rap1b*$^{-/-}$ platelets, with reductions of 89 and 86%, respectively, in comparison to vehicle-treated controls. The observation that LY-294002 further reduced the aggregation of Rap1b$^{-/-}$ platelets indicated that, even though Rap1b is involved in GPVI-mediated activation, it is not the only effector of PI3K in this response.

To elucidate the PI3K isoforms implicated in Rap1b activation directly downstream of GPVI, the effect of CRP was evaluated on Rap1b-GTP levels in platelets treated with autocrine stimulation inhibitors. An inhibitor of $\alpha_{IIb}\beta_3$ of human (40 μg/ml Reopro) or mouse (100 μM GPI-562) platelets served to suppress platelet aggregation, which process interferes with the assay. In both human and mouse platelets, CRP induced a potent activation of Rap1b (Fig. 9, *A* and *B*). Treatment with LY-294002 strongly suppressed Rap1b activation with Rap1-GTP levels being reduced in human and mouse platelets by 72 and 69%, respectively. Markedly, treatment with TGX-221 or PIK-75 resulted in a similar degree of reduction in Rap1b activation, both in mouse or human platelets. In contrast, effects of AS-252424 treatment were negligible. These findings demonstrate a major role for PI3Kα and -β but not -γ in Rap1b activation downstream of GPVI.

DISCUSSION

The present report provides the first data showing the contribution of multiple PI3K isoforms in GPVI-induced activation of (human) platelets and the role of these isoforms in GPVI-dependent thrombus formation. Our findings significantly extend the earlier evidence that GPVI agonists increase the formation of PI(3,4,5)P_3 and its derivative phosphoinositide 3,4-bisphosphate via PI3K activation (9, 10, 46). A marked finding is that both PI3Kα and -β isoforms are needed for full $InsP_3$ formation and Ca^{2+} signal generation, thus suggesting that both activities are necessary for optimal activation of the key effector enzyme of GPVI, PLCγ2. Detailed Ca^{2+} measurements in the presence of extracellular EGTA and $CaCl_2$ pointed to a marked contribution of PI3K to Ca^{2+} mobilization from intracellular stores, which is a direct read-out of PLC, and not to a (store-independent) effect on Ca^{2+} entry. Hence, the earlier suggested regulation of Ca^{2+} entry by PI3K or its product PI(3,4,5)P_3 (23, 24) seems to be secondary to the effect of PI3K regulation of Ca^{2+} store depletion.

Several observations point to a non-redundant contribution of PI3Kα and -β isoforms in GPVI-induced platelet activation. These include the inhibitory effects on human platelets of a panel of compounds with high affinity to PI3Kα (PIK-75, PI-103, and YM-024) or to PI3Kβ (TGX-221 and also PI-103). Other support comes from studies with mouse platelets, which responded similarly to the isoform-specific inhibitors as did human platelets. Furthermore, we found that mouse platelets lacking p85α were strikingly impaired in collagen-induced Ca^{2+} signaling and thrombus formation. These *p85*$\alpha^{-/-}$ platelets are fully depleted in p110α, but still express residual p85β and p110β (11). However, treatment of these platelets with TGX-221 did not further suppress Ca^{2+} signaling and downstream responses such as PS exposure, although this compound did insignificantly reduce *p85*$\alpha^{-/-}$ platelet deposition under flow. This suggested a function of the residual p110β in ADP-dependent platelet aggregate formation.

In human platelets, inhibition of PI3Kγ (AS-252424) failed to affect the GPVI-induced Ca^{2+} response, whereas inhibition of PI3Kδ (IC-87114) caused a minor reduction, in contrast to the marked effect of PI3Kα/β inhibition. Similarly, mouse platelets, which were deficient in p110γ or p110δ, showed undiminished activation, when stimulated with GPVI agonist under conditions where autocrine stimulators were blocked. These results are supported by data from others, showing that deficiency in murine *p110*γ (19) or *p110*δ (26) has no more than a modest role in GPVI-induced platelet activation.

FIGURE 7. **Murine p85α regulates collagen-induced Ca^{2+} responses and thrombus formation under flow.** PPACK/heparin-anti-coagulated blood from *p85*$\alpha^{+/+}$ or *p85*$\alpha^{-/-}$ mice, spiked with 10% Fluo-3-loaded platelets from the same mouse strain, was flowed over collagen at 1000 s^{-1}. The blood was preincubated with Me_2SO vehicle or TGX-221 (1 μM). *A*, contribution of p85α to Ca^{2+} responses under high shear perfusion. *Upper panels*: averaged overlays of $[Ca^{2+}]_i$ traces from >25 platelets; *lower panels*: traces from representative single platelets. *Bars* show quantification of $[Ca^{2+}]_i$ increases at 20 s (*gray*) or 60 s (*white*) after initial platelet activation. *B*, contribution of p85α to thrombus formation and PS exposure. Shown are representative images of phase-contrast (120 × 120 μm) and OG-annexin A5 fluorescence (150 × 150 μm) of *p85*$\alpha^{+/+}$ and *p85*$\alpha^{-/-}$ thrombi. *Bars* represent surface area coverage of all deposited platelets and PS-exposing platelets. *C* and *D*, effect of pharmacological PI3K inhibition on thrombus formation and PS exposure. Wild-type blood was preincubated with Me_2SO vehicle (control), PIK-75, TGX-221, or wortmannin (each 1 μM). Data are means ± S.E. ($n = 3$–5); *, $p < 0.05$ compared with vehicle control; #, $p < 0.05$ compared with wild type.

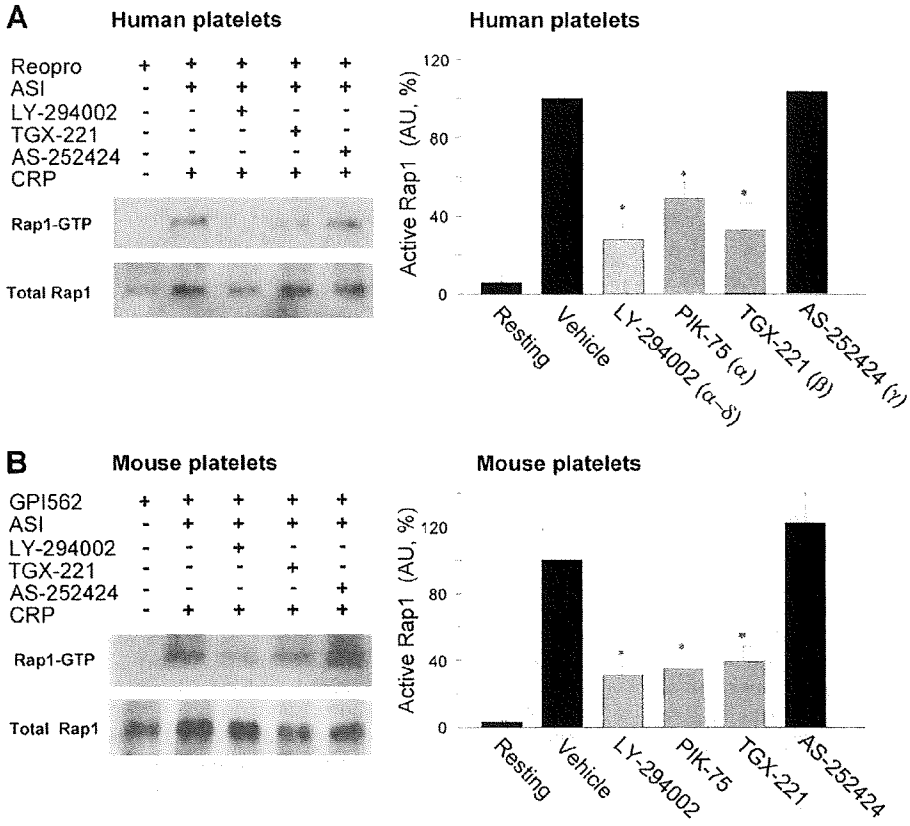

FIGURE 9. **Contribution of PI3K isoforms to GPVI-induced activation of Rap1b.** Washed human (*A*) and wild-type mouse (*B*) platelets (3×10^8/ml) were preincubated with autocrine stimulation inhibitors (*ASI*) (Fig. 8) and $\alpha_{IIb}\beta_3$ inhibitor (human: 40 μg/ml Reopro; mouse: 100 μM GPI-562). Incubations contained Me_2SO vehicle or PI3K inhibitor LY-294402 (25 μM), TGX-221 (0.5 μM), or AS-252424 (10 μM). Platelets were stimulated with 20 μg/ml CRP, lysed, and used for immunoprecipitation of GTP-Rap1. *A* and *B*, representative Western blots of active Rap1-GTP and total Rap1. *Right panels*: densitometric analysis of the amount of active Rap1-GTP (arbitrary units). Means ± S.E. (n = 3–5); *, $p < 0.05$ compared with control.

The role of PI3Kα and -β isoforms was particularly clear in measurements of GPVI-dependent thrombus formation, where platelets were flowed over collagen at a defined physiological shear rate. Blocking or deficiency in PI3Kα/β resulted in suppression of Ca^{2+} increases and PS exposure of platelets adhered to collagen, as well as in reduced formation of aggregate formation. For both human and mouse blood, it is known that these responses fully rely on GPVI signaling via Src family kinases to LAT and PLCγ2 (34, 47). Hence, the present findings support a concept that full PLCγ2-evoked activity is required for optimal platelet activation and thrombus formation under flow. Earlier, it was established that at the same flow conditions different populations of platelets assemble into aggregates or expose PS (38). Although this heterogeneity in platelet responses was maintained with PI3Kα/β inhibition or absence, the present results also suggest that the reduced PS exposure in inhibited platelets is a direct consequence of the reduced Ca^{2+} signal of those platelets that are adhered to collagen.

Earlier, we and others have shown that two PI3K isoforms, namely PI3Kβ and -γ, are implicated in ADP/$P2Y_{12}$-induced integrin $\alpha_{IIb}\beta_3$ activation and subsequent thrombus stabilization (17, 19, 20). Recently, these observations were extended to *in vivo* thrombosis models, where wortmannin treatment of *p110*γ-deficient mice was found to cause a dramatic defect in initial thrombus growth following vascular damage (21). The present data shed a new light on these *in vivo* observations, because it now appears that both collagen- and ADP-dependent platelet activation processes are affected by PI3K inhibition with a likely key role of the PI3Kα/β isoforms.

There is a growing body of evidence that, in many cell systems individual PI3K isoforms, although involved in specific cellular functions, show functional redundancy, *e.g.* as noted for the additive contribution of PI3Kβ and -γ in complement 5a-stimulated macrophages (48). So far, non-redundancy in PI3K function has been described only in particular cases. For example, in neutrophils producing inflammatory reactive oxygen species, both PI3Kγ and -δ isoforms contribute to $PI(3,4,5)P_3$ formation, but in this case the role of PI3Kγ may be prior to that of PI3Kδ (31, 49). In comparison to platelets, this is reminiscent of the early contribution of PI3Kα/β in GPVI stimulation, and the later involvement of PI3Kβ/γ in responses to autocrine produced ADP.

In the classic scheme of immunoglobulin receptor-linked PLCγ activity, as proposed for lymphocytes, accumulation of $PI(3,4,5)P_3$ in the plasma membrane may function as an anchoring site for the N-terminal pleckstrin homology domain of PLCγ isoforms (18, 50). This scheme can be applicable to GPVI-stimulated platelets as well. Given the high turnover of phosphoinositides in the platelet plasma membrane, we hypothesize that the stimulation and anchoring of PLCγ2 requires a threshold elevation of $PI(3,4,5)P_3$ that can only be achieved by simultaneous activity of PI3Kα and -β. In other words, activation of either PI3Kα or -β alone may be insufficient for PLCγ2 targeting to membrane via its PH domain. It is conceivable that this is a consequence of the need of PLCγ2 to compete with other PH-domain containing signaling proteins such as Akt isoforms. Such a mechanism would provide an attractive, but not the only, explanation for the identified non-redundant contribution to GPVI-induced signaling of both PI3K isoforms. One possible scenario is that one isoform may produce an initial small amount of $PI(3,4,5)P_3$, which in turn promotes activation of the other isoform through $PI(3,4,5)P_3$ regulation of p85 subunits. Future studies examining temporal signaling by individual PI3K isoforms, as previously performed in neutrophils (31), will be needed to address this issue. The enhancing effect of PI3K activity on PLCγ2 is in

contrast to the essential contribution of Src family kinases to GPVI-induced activation, because this is apparent from the complete abrogation of GPVI-induced Ca^{2+} increases by Src family kinase inhibition (39).

The literature contains solid evidence that platelet Rap1b is activated in a PI3K-dependent manner, in particular after occupation of G_i-coupled receptors such as the $P2Y_{12}$ receptor for ADP (27, 28). By using autocrine stimulation inhibitors, where the $P2Y_{12}$-dependent component was blocked, we could identify, for both human and mouse platelets, the existence of a direct GPVI-stimulated and PI3K-dependent component of Rap1b activation. Use of the isoform-specific inhibitors revealed involvement of PI3Kα/β in this activation of Rap1b. However, the prominent suppressive effect of PI3K inhibitors on $\alpha_{IIb}\beta_3$ activation and aggregation seen in *Rap1b*$^{-/-}$ platelets indicates that the PI3K isoforms contribute to GPVI-induced integrin activation also through a pathway that is independent of Rap1b. This pathway may involve PI3Kα/β-dependent stimulation of PLCγ2, which can contribute to the Ca^{2+}- and protein kinase C-mediated activation of $\alpha_{IIb}\beta_3$.

PI3Kα is the most frequently mutated kinase in human cancer. Hence, this isoform has raised great interest as a target for novel anti-tumor drugs, some of which are currently in early stage clinical trials (51). Given the likely important function of GPVI in (experimental) thrombosis, the present data suggest another important application for PI3Kα and PI3Kβ inhibitors, namely in anti-platelet therapy and arterial thrombosis. In this context, it is relevant to note that arterial thrombosis is a known companion of some cancers. The availability of selective pharmacological agents against specific isoforms may thus offer new potential approaches for prevention of these diseases.

Acknowledgments—We thank Dr. A. van Montfoort for performing preliminary experiments. We acknowledge the Baker Heart Research Institute (Melbourne, Australia) for the kind gift of PI3K isoform inhibitors.

Addendum—While this report was in revision, other authors have also reported that PIK3β plays an essential role in GPVI-induced activation of mouse platelets (52).

REFERENCES

1. Nieswandt, B., and Watson, S. P. (2003) *Blood* **102,** 449–461
2. Watson, S. P., and Gibbins, J. M. (1998) *Immunol. Today* **19,** 260–264
3. Heemskerk, J. W., Kuijpers, M. J., Munnix, I. C., and Siljander, P. R. (2005) *Trends Cardiovasc. Med.* **15,** 86–92
4. Jackson, S. P. (2007) *Blood* **109,** 5087–5095
5. Jandrot-Perrus, M., Lagrue, A. H., Okuma, M., and Bon, C. (1997) *J. Biol. Chem.* **272,** 27035–27041
6. Knight, C. G., Morton, L. F., Onley, D. J., Peachey, A. R., Ichinohe, T., Okuma, M., Farndale, R. W., and Barnes, M. J. (1999) *Cardiovasc. Res.* **41,** 450–457
7. Siljander, P., Farndale, R. W., Feijge, M. A., Comfurius, P., Kos, S., Bevers, E. M., and Heemskerk, J. W. (2001) *Arterioscler. Thromb. Vasc. Biol.* **21,** 618–627
8. Gibbins, J. M., Briddon, S., Shutes, A., van Vugt, M. J., van de Winkel, J. G., Saito, T., and Watson, S. P. (1998) *J. Biol. Chem.* **273,** 34437–34443
9. Lagrue, A. H., Francischetti, I. M., Guimarães, J. A., and Jandrot-Perrus, M. (1999) *FEBS Lett.* **448,** 95–100
10. Pasquet, J. M., Bobe, R., Gross, B., Gratacap, M. P., Tomlinson, M. G., Payrastre, B., and Watson, S. P. (1999) *Biochem. J.* **342,** 171–177
11. Watanabe, N., Nakajima, H., Suzuki, H., Oda, A., Matsubara, Y., Moroi, M., Terauchi, Y., Kadowaki, T., Suzuki, H., Koyasu, S., Ikeda, Y., and Handa, M. (2003) *Blood* **102,** 541–548
12. Stephens, L., Williams, R., and Hawkins, P. (2005) *Curr. Opin. Pharmacol.* **5,** 357–365
13. Rückle, T., Schwarz, M. K., and Rommel, C. (2006) *Nat. Rev. Drug Discov.* **5,** 913–918
14. Ali, K., Bilancio, A., Thomas, M., Pearce, W., Gilfillan, A. M., Tkaczyk, C., Kuehn, N., Gray, A., Giddings, J., Peskett, E., Fox, R., Bruce, I., Walker, C., Sawyer, C., Okkenhaug, K., Finan, P., and Vanhaesebroeck, B. (2004) *Nature* **431,** 1007–1011
15. Rittenhouse, S. E. (1996) *Blood* **88,** 4401–4414
16. Vanhaesebroeck, B., and Waterfield, M. D. (1999) *Exp. Cell Res.* **253,** 239–254
17. Jackson, S. P., Schoenwaelder, S. M., Goncalves, I., Nesbitt, W. S., Yap, C. L., Wright, C. E., Kenche, V., Anderson, K. E., Dopheide, S. M., Yuan, Y., Sturgeon, S. A., Prabaharan, H., Thompson, P. E., Smith, G. D., Shepherd, P. R., Daniele, N., Kulkarni, S., Abbott, B., Saylik, D., Jones, C., Lu, L., Giuliano, S., Hughan, S. C., Angus, J. A., Robertson, A. D., and Salem, H. H. (2005) *Nat. Med.* **11,** 507–514
18. Schlessinger, J. (2000) *Cell* **103,** 211–225
19. Hirsch, E., Bosco, O., Tropel, P., Laffargue, M., Calvez, R., Altruda, F., Wymann, M., and Montrucchio, G. (2001) *FASEB J.* **15,** 2019–2021
20. Cosemans, J. M., Munnix, I. C., Wetzker, R., Heller, R., Jackson, S. P., and Heemskerk, J. W. (2006) *Blood* **108,** 3045–3052
21. Schoenwaelder, S. M., Ono, A., Sturgeon, S., Chan, S. M., Mangin, P., Maxwell, M. J., Turnbull, S., Mulchandani, M., Anderson, K., Kauffenstein, G., Rewcastle, G. W., Kendall, J., Gachet, C., Salem, H. H., and Jackson, S. P. (2007) *J. Biol. Chem.* **282,** 28648–28658
22. Lecut, C., Schoolmeester, A., Kuijpers, M. J., Broers, J. L., van Zandvoort, M. A., Vanhoorelbeke, K., Deckmyn, H., Jandrot-Perrus, M., and Heemskerk, J. W. (2004) *Arterioscler. Thromb. Vasc. Biol.* **24,** 1727–1733
23. Pasquet, J. M., Quek, L., Stevens, C., Bobe, R., Huber, M., Duronio, V., Krystal, G., and Watson, S. P. (2000) *EMBO J.* **19,** 2793–2802
24. Lu, P. J., Hsu, A. L., Wang, D. S., and Chen, C. S. (1998) *Biochemistry* **37,** 9776–9783
25. Woulfe, D., Jiang, H., Morgans, A., Monks, R., Birnbaum, M., and Brass, L. F. (2004) *J. Clin. Invest.* **113,** 441–450
26. Senis, Y. A., Atkinson, B. T., Pearce, A. C., Wonerow, P., Auger, J. M., Okkenhaug, K., Pearce, W., Vigorito, E., Vanhaesebroeck, B., Turner, M., and Watson, S. P. (2005) *Platelets* **16,** 191–202
27. Lova, P., Paganini, S., Hirsch, E., Barberis, L., Wymann, M., Sinigaglia, F., Balduini, C., and Torti, M. (2003) *J. Biol. Chem.* **278,** 131–138
28. Woulfe, D., Jiang, H., Mortensen, R., Yang, J., and Brass, L. F. (2002) *J. Biol. Chem.* **277,** 23382–23390
29. Suzuki, H., Terauchi, Y., Fujiwara, M., Aizawa, S., Yazaki, Y., Kadowaki, T., and Koyasu, S. (1999) *Science* **283,** 390–392
30. Chrzanowska-Wodnicka, M., Smyth, S. S., Schoenwaelder, S. M., Fischer, T. H., and White, G. C., 2nd (2005) *J. Clin. Invest.* **115,** 680–687
31. Condliffe, A. M., Davidson, K., Anderson, K. E., Ellson, C. D., Crabbe, T., Okkenhaug, K., Vanhaesebroeck, B., Turner, M., Webb, L., Wymann, M. P., Hirsch, E., Ruckle, T., Camps, M., Rommel, C., Jackson, S. P., Chilvers, E. R., Stephens, L. R., and Hawkins, P. T. (2005) *Blood* **106,** 1432–1440
32. Kuijpers, M. J., Schulte, V., Bergmeier, W., Lindhout, T., Brakebusch, C., Offermanns, S., Fässler, R., Heemskerk, J. W., and Nieswandt, B. (2003) *FASEB J.* **17,** 685–687
33. Maxwell, M. J., Yuan, Y., Anderson, K. E., Hibbs, M. L., Salem, H. H., and Jackson, S. P. (2004) *J. Biol. Chem.* **279,** 32196–32204
34. Siljander, P. R., Munnix, I. C., Smethurst, P. A., Deckmyn, H., Lindhout, T., Ouwehand, W. H., Farndale, R. W., and Heemskerk, J. W. (2004) *Blood* **103,** 1333–1341
35. Feijge, M. A., van Pampus, E. C., Lacabaratz-Porret, C., Hamulyàk, K., Levy-Toledano, S., Enouf, J., and Heemskerk, J. W. (1998) *Br. J. Haematol.* **102,** 850–859
36. Heemskerk, J. W., Feijge, M. A., Henneman, L., Rosing, J., and Hemker, H. C. (1997) *Eur. J. Biochem.* **249,** 547–555
37. Cauwenberghs, S., Feijge, M. A., Theunissen, E., Heemskerk, J. W., van

Pampus, E. C., and Curvers, J. (2007) *Br. J. Haematol.* **136,** 480–490
38. Munnix, I. C., Kuijpers, M. J., Auger, J., Thomassen, C. M., Panizzi, P., van Zandvoort, M. A., Rosing, J., Bock, P. E., Watson, S. P., and Heemskerk, J. W. (2007) *Arterioscler. Thromb. Vasc. Biol.* **27,** 2484–2490
39. Auger, J. M., Kuijpers, M. J., Senis, Y. A., Watson, S. P., and Heemskerk, J. W. (2005) *FASEB J.* **19,** 825–827
40. Heemskerk, J. W., Willems, G. M., Rook, M. B., and Sage, S. O. (2001) *J. Physiol.* **535,** 625–635
41. Chaussade, C., Rewcastle, G. W., Kendall, J. D., Denny, W. A., Cho, K., Gronning, L. M., Chong, M. L., Anagnostou, S. H., Jackson, S. P., Daniele, N., and Shepherd, P. R. (2007) *Biochem. J.* **404,** 449–458
42. Kim, S., Garcia, A., Jackson, S. P., and Kunapuli, S. P. (2007) *Blood* **110,** 4206–4213
43. Savage, B., Ginsberg, M. H., and Ruggeri, Z. M. (1999) *Blood* **94,** 2704–2715
44. Nesbitt, W. S., Mangin, P., Salem, H. H., and Jackson, S. P. (2006) *J. Mol. Med.* **84,** 989–995
45. Terauchi, Y., Tsuji, Y., Satoh, S., Minoura, H., Murakami, K., Okuno, A., Inukai, K., Asano, T., Kaburagi, Y., Ueki, K., Nakajima, H., Hanafusa, T., Matsuzawa, Y., Sekihara, H., Yin, Y., Barrett, J. C., Oda, H., Ishikawa, T., Akanuma, Y., Komuro, I., Suzuki, M., Yamamura, K., Kodama, T., Suzuki, H., Yamamura, K., Kodama, T., Suzuki, H., Koyasu, S., Aizawa, S., Tobe, K., Fukui, Y., Yazaki, Y., and Kadowaki, T. (1999) *Nat. Genet.* **21,** 230–235
46. Falet, H., Barkalow, K. L., Pivniouk, V. I., Barnes, M. J., Geha, R. S., and Hartwig, J. H. (2000) *Blood* **96,** 3786–3792
47. Nieswandt, B., Bergmeier, W., Eckly, A., Schulte, V., Ohlmann, P., Cazenave, J. P., Zirngibl, H., Offermanns, S., and Gachet, C. (2001) *Blood* **97,** 3829–3835
48. Guillermet-Guibert, J., Bjorklof, K., Salpekar, A., Gonella, C., Ramadani, F., Bilancio, A., Meek, S., Smith, A. J., Okkenhaug, K., and Vanhaesebroeck, B. (2008) *Proc. Natl. Acad. Sci. U.S.A.* **105,** 8292–8297
49. Suire, S., Condliffe, A. M., Ferguson, G. J., Ellson, C. D., Guillou, H., Davidson, K., Welch, H., Coadwell, J., Turner, M., Chilvers, E. R., Hawkins, P. T., and Stephens, L. (2006) *Nat. Cell Biol.* **11,** 1303–1309
50. Scharenberg, A. M., and Kinet, J. P. (1998) *Cell* **94,** 5–8
51. Vogt, P. K. (2008) *Cancer Cell* **14,** 107–108
52. Canobbio, I., Stefanini, L., Cipolla, L., Ciraolo, E., Gruppi, C., Balduini, C., Hirsch, E., and Torti, M. (2009) *Blood* **114,** 2193–2196